ФИЗИКА ЭЛЕМЕНТАРНЫХ ЧАСТИЦ И АТОМНОГО ЯДРА
2008. Т. 39. ВЫП. 2

INTERACTIONS OF RELATIVISTIC HEAVY IONS IN THICK HEAVY-ELEMENT TARGETS AND SOME UNRESOLVED PROBLEMS

R. Brandt [1,*], *V. A. Ditlov* [2], *K. K. Dwivedi* [3], *W. Ensinger* [1,4], *E. Ganssauge* [5], *Guo Shi-Lun* [6], *M. Haiduc* [7], *S. R. Hashemi-Nezhad* [8], *H. A. Khan* [9], *M. I. Krivopustov* [10], *R. Odoj* [11], *E. A. Pozharova* [2], *V. A. Smirnitzki* [2], *A. N. Sosnin* [10], *W. Westmeier* [1,12], *M. Zamani-Valasiadou* [13]

[1]Kernchemie, Fachbereich Chemie, Philipps-Universität, Marburg, Germany
[2]Institute for Theoretical and Experimental Physics, Moscow
[3]Embassy of India, Washington, DC, USA
[4]Institut für Materialwissenschaften, Technische Hochschule, Darmstadt, Germany
[5]Fachbereich Physik, Philipps-Universität, Marburg, Germany
[6]China Institute for Atomic Energy, Beijing
[7]Institute of Space Sciences, Bucharest
[8]Department of High Energy Physics, School of Physics, University of Sydney, Sydney, Australia
[9]COMSATS, Commission on Science and Technology for Sustainable Development in the South, Islamabad, Pakistan
[10]Joint Institute for Nuclear Research, Dubna
[11]Institut für Sicherheitsforschung, Forschungszentrum Jülich, Germany
[12]Gesellshaft für Kernspektrometrie, Ebsdorfergrund–Marburg, Germany
[13]Physics Department, Aristotle University, Thessaloniki, Greece

*Corresponding author.

ФИЗИКА ЭЛЕМЕНТАРНЫХ ЧАСТИЦ И АТОМНОГО ЯДРА
2008. Т. 39. ВЫП. 2

INTERACTIONS OF RELATIVISTIC HEAVY IONS IN THICK HEAVY-ELEMENT TARGETS AND SOME UNRESOLVED PROBLEMS

R. Brandt [1,*], *V. A. Ditlov* [2], *K. K. Dwivedi* [3], *W. Ensinger* [1,4], *E. Ganssauge* [5], *Guo Shi-Lun* [6], *M. Haiduc* [7], *S. R. Hashemi-Nezhad* [8], *H. A. Khan* [9], *M. I. Krivopustov* [10], *R. Odoj* [11], *E. A. Pozharova* [2], *V. A. Smirnitzki* [2], *A. N. Sosnin* [10], *W. Westmeier* [1,12], *M. Zamani-Valasiadou* [13]

[1]Kernchemie, Fachbereich Chemie, Philipps-Universität, Marburg, Germany
[2]Institute for Theoretical and Experimental Physics, Moscow
[3]Embassy of India, Washington, DC, USA
[4]Institut für Materialwissenschaften, Technische Hochschule, Darmstadt, Germany
[5]Fachbereich Physik, Philipps-Universität, Marburg, Germany
[6]China Institute for Atomic Energy, Beijing
[7]Institute of Space Sciences, Bucharest
[8]Department of High Energy Physics, School of Physics, University of Sydney, Sydney, Australia
[9]COMSATS, Commission on Science and Technology for Sustainable Development in the South, Islamabad, Pakistan
[10]Joint Institute for Nuclear Research, Dubna
[11]Institut für Sicherheitsforschung, Forschungszentrum Jülich, Germany
[12]Gesellshaft für Kernspektrometrie, Ebsdorfergrund–Marburg, Germany
[13]Physics Department, Aristotle University, Thessaloniki, Greece

Interactions of relativistic heavy ions with total energies above 30 GeV in thick Cu and Pb targets ($\geqslant$ 2 cm) have been studied with various techniques. Radiochemical irradiation experiments using thick Cu targets, both in a compact form or as diluted «2π-Cu targets», have been carried out with several relativistic heavy ions, such as 44 GeV ^{12}C (JINR, Dubna) and 72 GeV ^{40}Ar (LBL, Berkeley, USA). Neutron measuring experiments using thick targets irradiated with various relativistic heavy ions up to 44 GeV ^{12}C have been performed at the JINR. In addition, the number of «black prongs» in nuclear interactions (due to protons with energies less than 30 MeV and emitted from the target-like interaction partner at rest) produced with 72 GeV ^{22}Ne ions in nuclear emulsion plates has been measured in the first nuclear interaction of the primary ^{22}Ne ions and in the following second nuclear interaction of the secondary heavy ($Z > 1$) ions. Some essential results have

*Corresponding author.

been obtained. 1) Spallation products produced by relativistic secondary fragments in interactions ([44 GeV ^{12}C or 72 GeV ^{40}Ar] + Cu) within thick copper yield less products close to the target and much more products far away from the target as compared to primary beam interactions. This applies also to secondary particles emitted at large angles ($\Theta > 10^\circ$). 2) The neutron production of 44 GeV ^{12}C within thick Cu and Pb targets is beyond the estimated yield as based on experiments with 12 GeV ^{12}C. These rather independent experimental results cannot be understood with well-accepted nuclear reaction models. They appear to present unresolved problems.

Взаимодействия релятивистских тяжелых ионов с полной энергией, превышающей 30 ГэВ, в протяженных медных и свинцовых мишенях ($\geqslant 2$ см) исследовались с применением различных методик. Радиохимические эксперименты по облучению толстых медных мишеней как в компактной конфигурации, так и в распределенной конфигурации «2π-Cu-мишени» проводились с различными релятивистскими тяжелыми ионами, такими как ^{12}C с энергией 44 ГэВ (ОИЯИ, Дубна) или ^{40}Ar с энергией 72 ГэВ (Беркли, США). Эксперименты по измерению нейтронных полей, генерируемых в толстых мишенях, облучаемых различными релятивистскими тяжелыми ионами вплоть до ^{12}C с энергией 44 ГэВ, были выполнены в ОИЯИ. В дополнение к этому измерялось количество «черных» следов в ядерных взаимодействиях (вызываемых протонами с энергией менее 30 МэВ во взаимодействиях с ядром-мишенью в состоянии покоя). Эти протоны генерируются ионами ^{22}Ne при энергии 72 ГэВ в пластинах ядерной эмульсии. Эти следы измерялись как для случая первого взаимодействия первичных ионов ^{22}Ne, так и для вторичных ядерных взаимодействий тяжелых ($Z > 1$) ионов. Приводятся некоторые существенные результаты. 1) Продукты расщепления, которые рождаются релятивистскими вторичными фрагментами во взаимодействиях ионов ^{12}C при 44 ГэВ или ^{40}Ar при 72 ГэВ с толстыми медными мишенями, приводят к рождению меньшего количества продуктов реакции в непосредственной близости от мишени, чем в случае больших расстояний от мишени, по сравнению с взаимодействиями первичного пучка. Этот вывод распространяется также на случай испускания вторичных частиц под большими углами ($\Theta > 10^\circ$). 2) Рождение нейтронов во взаимодействиях ионов ^{12}C с энергией 44 ГэВ в толстых медных и свинцовых мишенях превышает выход реакции, который можно ожидать по данным экспериментов с ионами углерода при энергии 12 ГэВ. Такие независимые экспериментальные результаты не могут быть объяснены в рамках принятых моделей ядерных реакций. По-видимому, они указывают на наличие нерешенных проблем.

PACS: 34.50.-s

INTRODUCTION

Some specific nuclear reactions induced by relativistic ions with total kinetic energies above 30 GeV have been reinvestigated. In particular, nuclear interactions were studied in thick targets with nuclear charges above $Z = 20$. Such thick targets were exposed to primary projectiles and their relativistic secondary fragments. The target could be metallic copper, lead, or even a nuclear emulsion based on AgBr embedded in a conventional low-Z emulsion containing H, C, N, and O atoms. The thickness of such a target could be 2 cm or more, ranging up to the total path of the primary ion within the target material. The problems to be discussed have recently attracted some fresh interest due to serious doubts about our complete understanding of nuclear interactions in thick targets [1]. The essential question is:

Do relativistic secondary fragments produced in relativistic nucleus–nucleus interactions react in the same manner with target nuclei as their relativistic primary «parent» projectiles?

This scientific problem has been known for more than 50 years, but it appears that it has never been studied in a systematic manner, so that the science community would accept the experimental findings together with model considerations to interpret these phenomena. This is particularly true for ideas not conforming with well-accepted concepts of physics. Four types of such phenomena will be studied in this paper.

• Some radiochemical evidences observed in yield distributions in thick and compact targets produced by relativistic secondary fragments appear to be outside the concept of «limiting fragmentation». The recent PhD thesis of Lerman [2] gives a fine account on the history of these investigations and it contains valuable contributions for the study of these problems using 72 GeV ^{40}Ar from the Bevalac at the Lawrence Berkeley Laboratory (USA). A similar recent study employing relativistic heavy ions up to 44 GeV ^{12}C from the Synchrophasotron at the Laboratory for High Energies (JINR, Dubna) has been published in the PhD thesis of Ochs [3]. Additional references will be given later.

• Similar radiochemical evidences have also been observed for interactions of wide-angle ($\Theta > 10^{\circ}$) emitted secondary particles produced with 44 GeV ^{12}C and 72 GeV ^{40}Ar in the irradiation of diluted «2π-Cu targets» (to be explained later in the text) [4–9].

• A strong more-than-linear enhancement with energy of secondary neutron production within the energy range from 12 up to 44 GeV for ^{12}C ions has been measured in irradiations of thick Pb targets. This phenomenon had been observed a long time ago by Vassilkov et al. [10]. The effect could not be observed for irradiations with relativistic p-, deuterium, and ^{4}He ions. These findings have been confirmed recently using other Cu- and Pb-target configurations [11, 12].

• Most recently, the excitation (i.e., destruction) of target nuclei through relativistic secondary heavy ($Z > 1$) fragments was studied in nuclear emulsion irradiated with 72 GeV ^{22}Ne ions. A measure for the destruction is the number of «black prongs» in a single nuclear interaction «star». The black-prong tracks are due to protons with energies less than 30 MeV that are evaporated from the target-like residual nucleus. In this paper, the number of black prongs, N_b, was measured in the *first* nuclear interaction, $^{1}N_b$, and also in the *second* nuclear interaction, $^{2}N_b$, along the ion tracks of 72 GeV ^{22}Ne in nuclear emulsion. Any observed enhancement in $^{2}N_b$ over $^{1}N_b$ could be an indication of «enhanced destruction potential» of the secondary fragments as compared to the primary particles. To our knowledge, this appears to be a new aspect in the experimental study of heavy-ion interactions in nuclear emulsions. It will be introduced into our discussions and first results will be presented [13].

A final summary of experimental results constituting several «unresolved problems» will be given. Two possible socio-economical applications, already given in [12], will be mentioned: 1) access to hitherto unknown energy reservoir and 2) information transfer in hitherto unknown media.

1. REACTION STUDIES IN THIN TARGETS: A SHORT REVIEW OF THE STATE-OF-ART

Before one can start a discussion of the potential observation of new phenomena in thick targets, it appears to be useful to recapitulate the state-of-art of our understanding of nuclear interactions induced by primary relativistic ions in thin targets. Respective experiments have been carried out for many decades, among others with radiochemical techniques and in nuclear emulsions.

Due to the earlier focus on nuclear interactions induced by primary ions only, one had measured the product yields in the so-called thin targets using radiochemical techniques. In this way one tried to minimize — and possibly exclude — contributions induced by secondary particles. The final result for decades of such radiochemical studies has been summarized by Cumming et al. [14]. Their concept of «limiting fragmentation» states:

The shape of the mass yield curve in a given target for target-like products is independent of the energy and mass of the projectile in nuclear interactions when irradiated with primary projectiles having a total energy above 1 GeV.

Their concept of «factorization» states:

The total reaction cross section increases with the mass of the projectile and target.

These concepts are demonstrated in Fig. 1 (taken from [14]) for the results of a series of experiments using thin Cu targets irradiated with 80 GeV ^{40}Ar, 25 GeV ^{12}C, and 28 GeV ^{1}H. A Cu target is considered as being thin, when only «primary» ions and almost no secondary fragments induce nuclear reactions. The shape of the mass yield curve is the same in all three irradiations, only the absolute interaction probability increases with the mass of the projectile. The qualitative physical interpretation is fairly simple and based on geometrical considerations only. The most likely nuclear interactions induced by relativistic ions are peripheral interactions where two nuclei overlap only slightly. Central collisions are much less likely. In a peripheral interaction, one has only little overlap of the nuclear wave functions resulting in little excitation and the emission of only a few nucleons. This shows up in the experimental observation that products close to the target are the most abundant reaction products as can be seen in Fig. 1. In more central collisions, there is an enhanced energy transfer and products further below the target mass can be produced. However, these are produced with much lower yield.

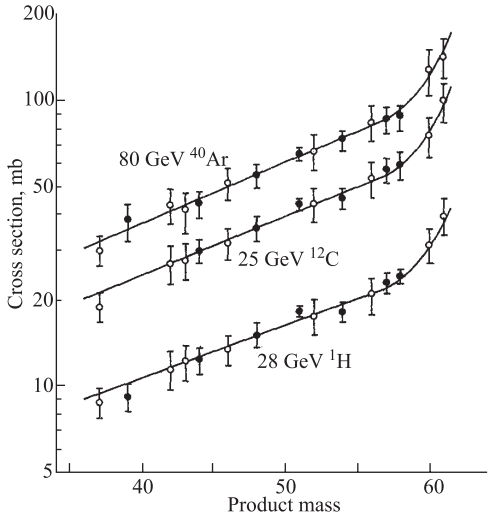

Fig. 1. Visual demonstration for the concepts of «limiting fragmentation» and «factorization» as observed in mass yield curves for thin Cu targets irradiated with 80 GeV ^{40}Ar, 25 GeV ^{12}C, or 28 GeV ^{1}H [14] (see details in the text)

Such nuclear interactions have not only been studied with radiochemical methods but also with nuclear emulsions irradiated with many different types of relativistic ions. As nuclear chemistry studies have been concentrated on *thin targets*, emulsion studies have been concentrated on the study of the *first nuclear interaction of an ion track inside the nuclear emulsion*. Consequently, one may expect equivalent scientific answers, in particular, a nearly exponential decrease of reaction products with increasing mass difference from the target nucleus. Such investigation was carried out by Friedlander and Friedman [15] in nuclear emulsions irradiated with relativistic protons with total energies above 1 GeV. They measured the number of «heavy prongs», N_h, in the first interactions along the trail of high-energy protons in nuclear emulsions. «Heavy prongs» are due to nuclear interactions of the primary proton with a nucleus of the emulsion. Each interaction yields an observeable «star» of tracks in the emulsion which becomes visible under an optical microscope. Quite abundant types of tracks are «heavy prongs» which are due to the emission of secondary protons from the excited target-like nucleus after the interaction with the primary proton. The kinetic energy of heavy-prong protons is in the range up to 400 MeV and they can be grouped into «black prongs»* having energies up to 30 MeV and «grey prongs»

*«Black prongs» will be investigated in detail in a later section of this paper.

with energies in the interval $30 < E_{\text{proton}} < 400$ MeV. It is obvious that more heavy prongs will be observed in a star when more energy has been deposited into the target nucleus — and vice versa — the smaller the number of heavy prongs, the lesser the destruction of the target nucleus. Friedlander and Friedman found out that the shape of the frequency distribution for N_h is independent of the irradiation energy. They observed the following quantitative result [quote]: «The log of the integral frequency distribution of N_h, $F(\geqslant N_h)$, is decreasing linearly with N_h^2. The decrease is independent of the energy of the protons with $E > 1$ GeV». The term, $F(\geqslant N_h)$, is defined as the number of N_h events larger or equal to N_h given for the actual ensemble of all interactions measured. This observation is an equivalent to the radiochemical observation of «limiting fragmentation» in thin targets. The result of their investigations is shown in Fig. 2. Figures 1 and 2 show the state-of-art for investigations in thin targets until about 1980.

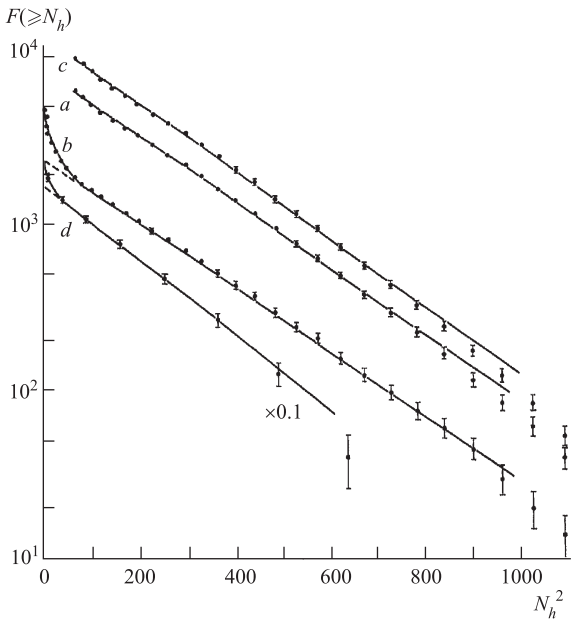

Fig. 2. Integral frequency distribution of «heavy prongs», N_h, in nuclear emulsions. *a*) 10 GeV protons (area scanning) for ($N_h \geqslant 9$); *b*) protons for all primary energies between 6 up to 2000 GeV (area scanning); *c*) all proton accelerator data for ($N_h \geqslant 8$); *d*) resulting distribution when subtracting *c* from *b*, all data taken from [15]. (The technical term «area scanning» is well known in the fields of emulsion studies and is described also in [15])

2. RADIOCHEMICAL STUDIES USING THICK AND COMPACT TARGETS

After extended studies using thin targets irradiated with primary relativistic ions in two separate fields of nuclear chemistry and nuclear emulsion techniques, a systematic study of the following question was initiated after 1980:

Do relativistic secondary projectile fragments interact in the same manner with target nuclei in thick targets as compared to their primary «parent» ion in thin targets?

Earlier investigations have been started 50 years ago in connection with the study of track lengths from relativistic primary ions as compared with their secondary fragments in nuclear emulsions. However, Friedlander and coworkers began about 1980 a systematic study of the track lengths of primary and relativistic secondary particles with $Z > 2$ in nuclear emulsions irradiated with 100 GeV ^{56}Fe ions from the Bevalac accelerator at the Lawrence Berkeley Laboratory (USA). They observed experimental evidence for a reduced mean free path of secondary fragments as compared to the mean free path of primary heavy ions. Their results have been published [16], however, these findings have not been accepted fully within the science community. As this specific field is discussed in a very controversial manner it shall not be discussed in this section. A fair review has been published by Ganssauge [17]. Recent evidence for a reduced mean free path of secondary fragments observed in cosmic rays was published by Dutta et al. [18] who suggested a new systematic way of discrimination between two complementary aspects in the investigation of these cm-range phenomena:

• Experiments focussing on a reduced mean free path of secondary fragments in the range from 1 to 10 cm suggest an *enhanced* ***total*** *nuclear cross section* for secondary fragments. (This effect was termed «physical anomalons» by Dutta et al. [18].)

• Experiments focussing on product yield distributions that go beyond the expectations of the concept of «limiting fragmentation» suggest effects due to *either enhanced — or reduced —* ***partial*** *nuclear cross sections,* within the same linear range as above. (This effect was termed «chemical anomalons» by Dutta et al. [18].)

The second class of interactions can be studied with radiochemical techniques using Cu targets, and such experiments were started about 1980 at the Bevalac accelerator of the Lawrence Berkeley Laboratory. These studies have been continued ever since using a variety of other accelerators. Substantial work was carried out at the Synchrophasotron accelerator of the Laboratory of High Energies (JINR, Dubna). We will start our presentation of radiochemical results in this paper with the JINR experiments. These radiochemical studies on thick Cu targets irradiated with different relativistic heavy ions are well documented, including technical details, in the PhD thesis of Ochs [3].

The 20 cm long target contained 20 Cu disks of 8 cm diameter and 1.0 cm thickness. A sketch of the target will be shown later in Fig. 15 and discussed together with further experiments. This target was irradiated with deuterium and ^{12}C ions in the kinetic energy range $3.0 \leqslant E_{\rm tot} \leqslant 44$ GeV from the Synchrophasotron with specific energies 1.5 and 3.7 GeV/A. After several hours of irradiation the induced radioactivity in the Cu disks was measured via gamma-ray spectrometry with HPGe counting systems. The production of four selected and typical reaction products, such as ^{24}Na, ^{43}K, ^{54}Mn, and ^{59}Fe, was determined quantitatively. Thus, production rates, $B(^{A}Z)$, of the isotopes ^{A}Z were directly measured in thick targets [3, 12]:

$$B(^{A}Z) = \frac{(\text{number of } {}^{A}Z \text{ atoms formed})}{[(1 \text{ g of Cu}) \cdot (1 \text{ primary ion})]}. \qquad (1)$$

The results of these studies are given in Fig. 3 for the selected number of Cu disks measured in all four heavy-ion irradiations: Due to limitations in the availability of gamma-counting capacity, only the 1st, 2nd, 4th, 6th, 8th, 10th, and 20th Cu disks were measured, and the sum of $B(^{A}Z)$ values for these measured seven Cu disks was determined. It is shown («sum of $B(^{A}Z)$ in seven copper disks» divided by «$B(^{A}Z)$ in the first Cu disk») in Fig. 3. This figure directly shows the amount of product nuclides in all seven Cu disks as compared to the first Cu disk for each isotope investigated.

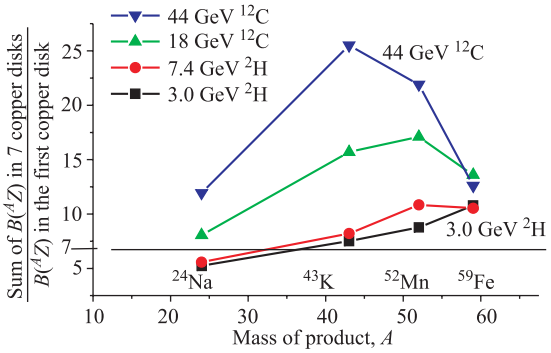

Fig. 3. Production rates $B(^{A}Z)$ of four nuclei (^{24}Na, ^{43}K, ^{52}Mn, ^{59}Fe) in seven Cu disks from a thick copper target consisting of 20 Cu disks (dimensions: 8 cm ∅, 1 cm thickness each) in the irradiation with relativistic deuterium and ^{12}C ions at different energies. The ordinate axis gives the ratio of the «sum of $B(^{A}Z)$ in seven Cu disks» divided by «$B(^{A}Z)$ in the first Cu disk». Each $B(^{A}Z)$ is measured with an uncertainty of ± 15%. Further details are given in the text

This representation was chosen for the following reason: It is known that only 14% of all ^{12}C ions are interacting in the first Cu disk [1]. Secondary fragments

may contribute also a little to the total production for any of the four investigated reaction products in this first Cu disk. In the other Cu disks further downstream, the relative production of reaction products due to secondary fragment reactions as compared to the primary ions must increase. This «sum of $B(^{A}Z)$ in seven copper disks compared to $B(^{A}Z)$ in the first Cu disk» thus gives a direct measure for the relative contribution of secondary fragments producing a reaction product as compared to primary ions. The «sum of $B(^{A}Z)$ in seven copper disks» is necessarily produced by interactions of primary ions plus secondary (and further) reaction products.

Following the concept of «limiting fragmentation», one knows relativistic ions with energies above 1 GeV (total kinetic energy, E_{tot}) and whichever nuclear charge yield product mass distributions in thin Cu targets of the shape as shown in Fig. 1. The maximum yield is observed for mass 59 (determined via ^{59}Fe, a spallation product close to the target nuclei ^{63,65}Cu), the spallation product ^{52}Mn is produced with a lower yield, the nuclide ^{43}K with an even lower yield. This comes from the fact that for larger mass difference from the target nucleus more energy is needed to produce such nuclei through evaporation. The fragmentation product ^{24}Na is produced with the lowest yield of all investigated products. The shape of the observed mass yield curve for 3.0 GeV deuterium irradiation of the thick 20 cm long Cu target conforms qualitatively with this expectation (see Fig. 3).

However, in studies of the mass yield curve for 44 GeV ^{12}C in the same target system, one observes a completely different behavior. There is maximum yield for ^{43}K, less yield for ^{59}Fe, and a considerably enhanced yield for the fragmentation product ^{24}Na is found. What is the reason for this different behavior of 44 GeV ^{12}C in a thick Cu target as compared to a thin Cu target? The only difference in these two Cu target systems is the fact that in thick Cu targets, in addition to primary ions, all secondary reaction products can induce additional nuclear interactions. Without going into further details here (it will be done later), it can be seen that secondary fragments (or maybe a considerable fraction of them) excite target nuclei stronger than primary 44 GeV ^{12}C ions do.

This may be deduced from the experimental fact that considerably more reaction products are formed in the thick Cu target with large ΔA as compared to a small ΔA ($\Delta A = A_{\mathrm{targ}} - A_{\mathrm{prod}}$). These observed effects apparently contradict the «limiting fragmentation» concept. From Fig. 3 it is furtheron clear that the yield disribution of the 7.4 GeV deuterium and 18 GeV ^{12}C is intermediate between the two extreme cases. One observes *an effect, which scales with the beam energy,* E_{tot}, of the primary ion. Such a behavior will be discussed with respect to other observed properties of these reactions in Sec. 3.

The presentation in Fig. 3 clearly shows the effect of secondary fragments on the ratios for the production of individual product isotopes ^{A}Z, in particular, for irradiations with 44 GeV ^{12}C on a 20 cm thick copper target. The absolute values

for the $B(A)$ distributions are not given in Fig. 3. ($B(A)$ is the product yield for all isotopes with mass A and it is also called «cumulative yield», $B(^{A}Z)$ gives the product yield for a specific isotope and in radiochemical terms it is called «independent yield».) Therefore, an additional presentation of the results for the product mass distribution has been chosen. The directly observed values, $B(A)$, for the product mass distribution are shown in Fig. 4 for the first and second Cu disks and for irradiations at both, the lowest energy (3 GeV deuterium, Fig. 4, *a*) and the highest irradiation energy (44 GeV ^{12}C, Fig. 4, *b*). Absolute values for

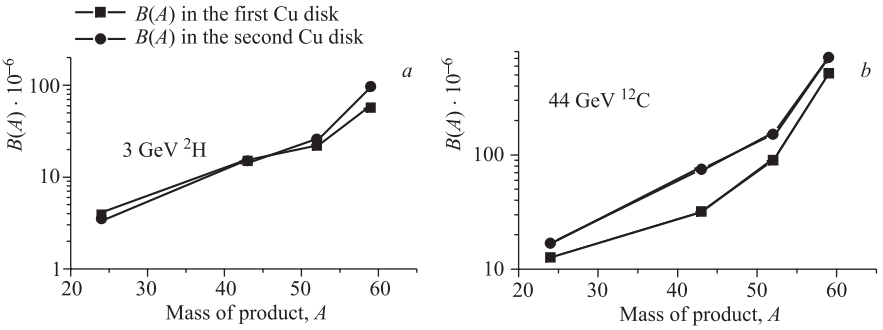

Fig. 4. The mass yields $B(A)$ for masses 24, 43, 52, and 59 produced with 3 GeV deuterium (*a*) and 44 GeV ^{12}C (*b*) in the first and second Cu disks

the cumulative mass yield $B(A)$ in the mass chains 24, 43, 52, and 59 are also given. We used standard radiochemical techniques for the conversion of the measured $B(^{59}\mathrm{Fe})$ — as an example — into the total chain yield $B(59)$. The experimental charge distribution curve was taken from Cumming et al. [14] for 80 GeV ^{40}Ar and 28 GeV p. The same charge distribution is assumed to hold also for our studies of primary and secondary fragments. The following results were observed.

3 GeV deuterium (Fig. 4, *a*). The $B(A)$ distributions in the first and second Cu disks are rather similar. Actually, the ratio $B(A)_{\mathrm{second}}/B(A)_{\mathrm{prim}}$ is close to unity for all product masses 24, 43, and 52 (see Table 1). No special increase due to secondary fragments is observed. Only $B(59)$ increases by $(70 \pm 26)\%$ when going from the first to the second Cu disk. This pattern can be well understood from calculated energy spectra for secondary protons and neutrons in the interaction of 2 GeV deuterium with the 1 cm thick Cu target. The computer program «MCNPX 2.5.e» [19] was used to calculate data for Fig. 5.

Only 0.59 protons and 0.87 neutrons are produced as secondary particles by one deuterium ion of 3 GeV. Most of the neutrons (85%) and many protons (44%) are produced with energies below 200 MeV. Secondary pions are produced in much smaller yields ($0.06\,\pi^{\pm}$ per ion), the heavier secondaries with even smaller yields ($< 10^{-3}$ per ion). All these secondaries produce predominantly spallation

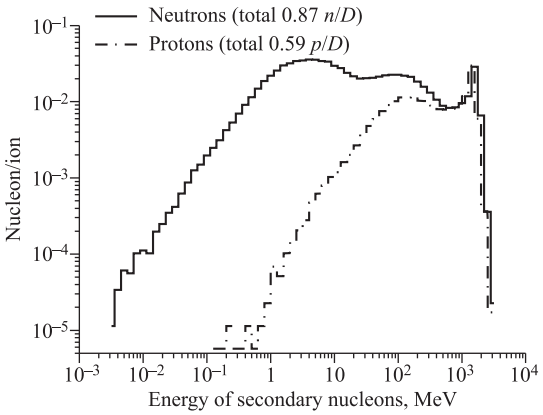

Fig. 5. The energy spectrum of the secondary nucleons produced by irradiation of a thin copper target ($L = 1$ cm, $\varnothing = 8$ cm) with 3 GeV deuterons. The plot is presented in equal logarithmic energy bins (10 intervals per decade)

products close to the target. Consequently, one can understand qualitatively that only spallation products close to the target like ^{59}Fe are produced with an appreciable $(70 \pm 26)\%$ increase in the second Cu disk.

44 GeV ^{12}C (Fig. 4, *b*). Here one observes a qualitatively different behavior. The $B(A)$ values are significantly larger in the second disk as compared to the first disk. A detailed analysis shows two further distinct differences. The $B(A)$ values for masses 43 and 52 are larger by a factor of 2.2 ± 0.3 in the second disk, whereas the increase is only a factor of 1.35 ± 0.15 for masses 24 and 59. These results qualitatively confirming observations were presented in Fig. 3. At present, we have no energy spectra for secondary particles produced in the interaction of 44 GeV ^{12}C with thin Cu targets in such a suitable form available for deuterium. Only some fragmentary calculations have been reported, so far [6]. Consequently, we turn to complementing experiments at the LBL in Berkeley, where experimental data and suitable calculations are available for the interaction of 72 GeV ^{40}Ar with Cu.

Similar radiochemical effects – in particular the enhanced excitation ability of secondary fragments as compared to beam ions — have been observed at the Bevalac accelerator in Berkeley during experiments starting about 1980 with relativistic ^{40}Ar ions. In these first experiments, only two Cu disks of 1.0 cm thickness and 8 cm diameter were irradiated for a few hours: In the first irradiation both Cu disks were in contact. In the following irradiation, the second Cu disk was separated from the first one by 20 cm downstream the beam direction. This experimental set-up is shown in Fig. 6. After the irradiation, the induced gamma activity was assayed and the yields for a large variety of product nuclides were

Table 1. **The ratio ($B(A)$ in the second Cu disk)/($B(A)$ in the first Cu disk), ($B(A)_{\rm second}/B(A)_{\rm prim}$), in three irradiations for four product masses A**

Product mass A	$B(A)_{\rm second}/B(A)_{\rm prim}$		
	3 GeV ^{2}H*	44 GeV ^{12}C*	72 GeV ^{40}Ar**
24	0.92 ± 0.05	1.33 ± 0.10	1.50 ± 0.02
43	0.97 ± 0.07	2.34 ± 0.19	2.05 ± 0.07
52	1.18 ± 0.18	2.08 ± 0.25	2.35 ± 0.05
59	1.70 ± 0.26	1.38 ± 0.16	1.79 ± 0.02

* The 3 GeV deuterium and 44 GeV ^{12}C experiments were carried out at the JINR.

** The 72 GeV ^{40}Ar experiment was carried out at the LBL.

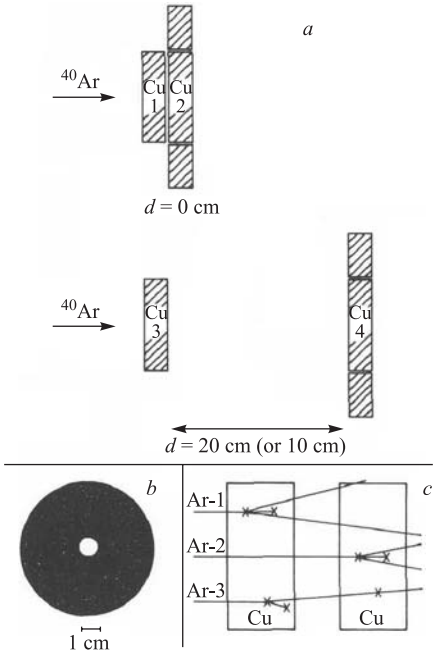

Fig. 6. The original two-Cu-disks experiments were carried out with relativistic ^{40}Ar ions at the Bevalac accelerator in Berkeley and started about 1980 [20, 21]. *a*) Schematic representation of the target set-up using two Cu disks and a surrounding guard ring around the second disk. *b*) Autoradiographic picture of a Cu disk after an irradiation with 72 GeV ^{40}Ar. *c*) Schematic representation of different reaction paths in the two Cu disks. Further details are given in [20, 21]

determined. In order to avoid uncertainties due to the determination of absolute production rates for specific isotopes, $B(^{A}Z)$, we focussed our attention in these earlier experiments only on the determination of cross-section ratios R_d, defined for a specific isotope ^{A}Z, where d is the distance between two Cu disks:

$$R_d(^{A}Z) = \frac{[B(^{A}Z) \text{ in the downstream Cu disk}]}{[B(^{A}Z) \text{ in the upstream Cu disk}]}. \qquad (2)$$

The irradiations were carried out with 72 and 36 GeV ^{40}Ar ions. $R_0(^AZ)$ was determined for two Cu disks in contact; and $R_{20}(^AZ)$, for two Cu disks separated by 20 cm. The results are shown in Fig. 7 and can be described as follows:

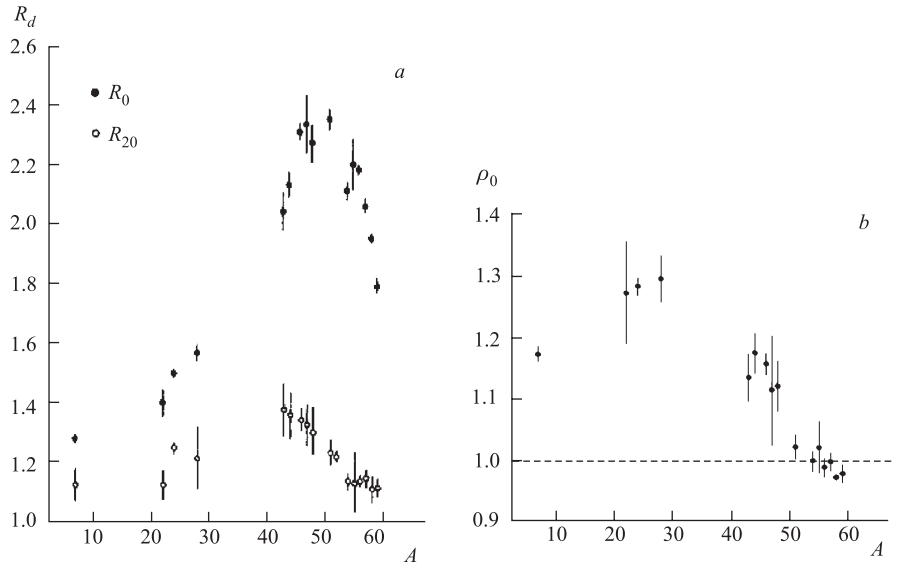

Fig. 7. *a*) The $R_d(^AZ)$ ratios for reaction products measured in two Cu disks and irradiated with 72 GeV ^{40}Ar. The distance between the two Cu disks was $d = 0$ cm for R_0 and $d = 20$ cm for R_{20}. These ratios can be determined quite accurately, similar to results in high-energy counter experiments [20, 21]. *b*) The dependence of the ratio $\rho_0 = R_0(A)_{(72\,\mathrm{GeV})}/R_0(A)_{(36\,\mathrm{GeV})}$ for Ar ions is shown as a function of the product mass number A [21]. Details are given in the text

• Figure 7, *a*. The distribution of $R_0(^AZ)$ for 72 GeV ^{40}Ar irradiations is shown for two Cu disks in contact and for all measured products with masses A in the range $7 \leqslant A \leqslant 59$. For $A = 7$ (^{7}Be) one measures $R_0(^7\mathrm{Be}) = 1.28 \pm 0.02$, then $R_0(^AZ)$ increases to about mass $A = 50$ with a maximum around $R_0(^{51}\mathrm{Cr}) = 2.35 \pm 0.04$ and then it decreases again towards higher masses up to mass 59 with $R_0(^{59}\mathrm{Fe}) = 1.79 \pm 0.03$. The original papers on this subject [20, 21] were concentrated almost exclusively on the interpretation of the experimental value for $R_0^{\mathrm{exp}}(^{24}\mathrm{Na}) = 1.50 \pm 0.02$. This value was experimentally determined with high accuracy and the excitation function for the production of ^{24}Na from thin Cu targets is very well known for protons in the energy range 300 MeV $< E_p <$ 300 GeV and also for many other heavy-ion induced reactions.

Knowing the yields and energy spectra of secondary fragments for the reaction in a thin Cu target irradiated with 72 GeV ^{40}Ar we can calculate the theoretical value $R_0^{\rm calc}(^{24}{\rm Na})$. L. Lerman [2] recently showed quite convincingly that the most advanced analysis — including the proper model calculations — for this experiment gives a theoretical value for $R_0^{\rm calc}(^{24}{\rm Na}) = 1.00 \pm 0.02$. The difference $[R_0^{\rm exp}(^{24}{\rm Na}) - R_0^{\rm calc}(^{24}{\rm Na}) = 0.50 \pm 0.03]$ is statistically very significant and it demonstrates a serious lack in our understanding of nuclear reactions induced by relativistic secondary fragments. This is another aspect of unresolved problems. Further details about results from [2] will be given later.

The representation of $R_{20}(^AZ)$ is also given in Fig. 7, *a* for cross-section ratios in two Cu disks separated by a distance $d = 20$ cm. The second Cu disk registers only secondary fragments emitted into the forward cone with the angle $\Theta_{\rm lab} < 11^\circ$. The $R_{20}(^AZ)$ values are smaller than $R_0(^AZ)$ values for all isotopes ^AZ between masses $A = 7$ and $A = 59$. There is evidence that these products are produced by secondary fragments emitted not only into a narrow forward angular cone but also into larger angles with $\Theta_{\rm lab} > 11^\circ$, as these isotopes are also observed in the Cu rings (see Fig. 6) surrounding the downstream Cu disk at $d = 20$ cm [21]. Quantitative results will be shown in Table 4 later.

• Figure 7, *b*. The $R_0(^AZ)$ distribution in irradiations of copper with 72 GeV ^{40}Ar ions is compared with those obtained with 36 GeV ^{40}Ar ions. The ratio $\rho_0 = R_0(A)_{(72\,{\rm GeV})}/R_0(A)_{(36\,{\rm GeV})}$ for Ar ions is shown as a function of the product mass A. At the larger Ar-ion energy essentially only nuclides with lower masses in the interval $7 \leqslant A \leqslant 50$ are produced with an enhanced yield, but for heavier masses $50 < A < 60$ production rates are constant. The maximum of the observed enhancement occurs around the nuclide ^{24}Na. Again, no model calculation is known to the authors, which can reproduce the experimental observation. This constitutes a further aspect of unresolved problems in this paper.

Another relevant question is: How does the experimental mass yield curve looks like in the second Cu disk as compared to the first Cu disk at a distance of $d = 0$ cm in irradiations with 72 GeV ^{40}Ar? The mass yield curve in the first Cu disk produced in this irradiation is unknown at present. In our experiments only the ratios for $R_0(^AZ)$ were experimentally determined [20, 21]. However, one can assume that due to the concept of «limiting fragmentation» the experimental mass yield curve for a thin Cu target produced by 1 GeV ^{12}C is approximately the same for 72 GeV ^{40}Ar interactions in the first Cu disk. Such a «reference mass yield curve» for 1 GeV ^{12}C beams [22] in copper was measured in great detail extending down to product masses of $A = 7$. This approximation of the mass yield curve for 72 GeV ^{40}Ar by the mass yield curve of 1 GeV ^{12}C is certainly a rather bold approximation. However, we have no better choice and for the argument under consideration (comparison of the mass yield curves with the second Cu disk and the first Cu disk) this approximation is quite sufficient.

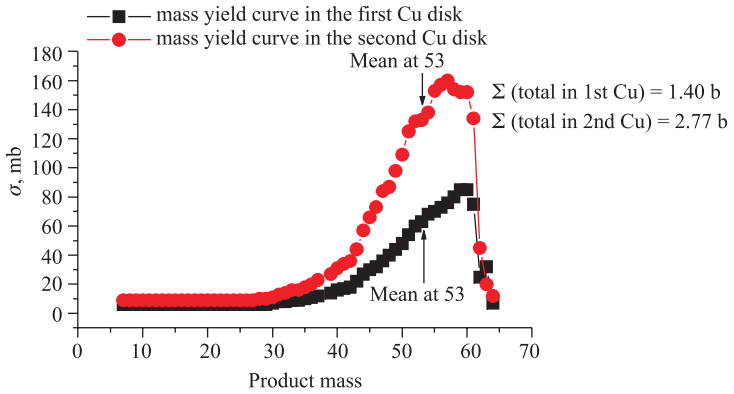

Fig. 8. The experimental mass yield curves in the first Cu disk assumed to be induced by primary 72 GeV ^{40}Ar ions [1, 22] only and in the second Cu disk induced by the same primary beam plus secondary fragments produced in the first Cu disk. Both Cu disks have been in contact. *Note*: The unknown mass yield curve produced by 72 GeV ^{40}Ar is approximated by the experimentally observed mass yield curve produced by 1 GeV ^{12}C. This is a valid approximation due to the concept of «limiting fragmentation». Details are given in the text

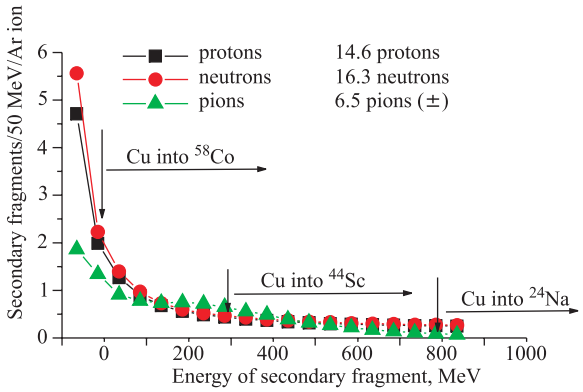

Fig. 9. Calculated energy spectra for secondary protons, neutrons, and pions produced by 72 GeV ^{40}Ar in a thin Cu target, using the Dubna DCM code [23]. For details see the text

This comparison of the mass yield curves in the first Cu disk and in the second Cu disk is shown in Fig. 8 for irradiations with 72 GeV ^{40}Ar. The construction of the mass yield curve within the second Cu disk is straightforward taking the increase in the production for each individual nuclear mass from the $R_0^{\exp}(^A Z)$ distribution shown in Fig. 7, *a*. The most striking result of this comparison is the apparently rather similar shape of both distributions, showing up as the same

mean value of both distributions at the mass $m = 53$. The increase in the yields for produced masses occurs mostly around mass 50 — just reflecting the results of the $R_0^{\exp}({}^A Z)$ distribution in Fig. 7, *a*. This lack of «special increases» in product masses close to $m = 59$ has already been shown in Table 1 and will be discussed below. The individual cross sections σ for a given mass A as well as the total cross-section sum Σ integrated over all masses are given in Fig. 8 as «appearent cross sections» normalized to the primary Ar-ion fluence.

Figure 8 should be interpreted on the basis of theoretical estimates of the energy spectra of secondary protons, neutrons, and pions. Model calculations have been carried out using the Dubna Cascade Code (DCM) [23]. The result of such a calculation for 72 GeV ^{40}Ar ions onto a thin Cu target is shown in Fig. 9 for secondary protons, neutrons, and pions. Most of these hadrons have energies below 200 MeV. About 23 energetic secondary hadrons (p, n, π) with energies $E > 50$ MeV are produced in a single interaction.

In order to obtain the first order estimate of the influence of these 23 secondaries (p, n, and π) on the production of spallation products in the second Cu disk, one can consider two aspects.

Approximate comparison of the total interaction cross-section sum in both Cu disks. It has been calculated that only 20% of all Ar ions interact within the first Cu disk and their kinetic energy is reduced only marginally [1]. Lerman could show, that nearly all Ar ions after the first interaction move on as projectile-like ions. They have charges $Z > 2$ and the same relative kinetic energy in terms of E/A as the primary projectile [2]. Consequently, 80% of primary Ar ions enter with almost primary energy into the second Cu disk together with these heavy projectile-like fragments. Assuming a «unit fluence» of primary Ar ions in the beginning, the total fluence of particles entering the second Cu disk is $(0.8 + 0.2 \cdot 23 = 5.4)$ times the «unit fluence». These p, n, and π have — provided they are relativistic with $E > 1$ GeV — only about 30% of the total interaction cross section as compared to 72 GeV ^{40}Ar as can be inferred from Fig. 1. Altogether one can roughly estimate that the «apparent» total interaction cross-section sum in the second Cu disk is $(0.8 + 4.6 \cdot 0.3) = 2.2$ times as much as in the first Cu disk. The observed cross-section ratio of $\Sigma^{\exp}(\text{total})_{\text{first disk}} = 1.40$ b divided by $\Sigma^{\exp}(\text{total})_{\text{second disk}} = 2.77$ b is 2.0 ($2.77 : 1.40 = 2.0$). However, in this very approximate estimate we have assumed relativistic energies above 1 GeV for all 23 secondary p, n, and π. Model calculations in Fig. 9 show definitely that about 70% of the secondary particles have energies below 400 MeV, thus being able only to produce spallation products heavier than ^{44}Sc. This order-of-magnitude estimate gives a somewhat satisfactory, but not a perfect agreement.

The influence of low-energy secondary *p, n,* and π. Calculations show that the majority of all secondaries have an energy below 200 MeV. The threshold for the production of ^{58}Co from Cu is around 100 MeV, for the production of ^{44}Sc

from Cu it is around 400 MeV [2], and the threshold for the production of ^{24}Na from Cu is around 900 MeV [20, 21]. This shows conclusively that low-energy secondaries will produce abundantly spallation products with masses above 55 in copper targets. The same conclusion is drawn from the textbook (Fig. 10). Here

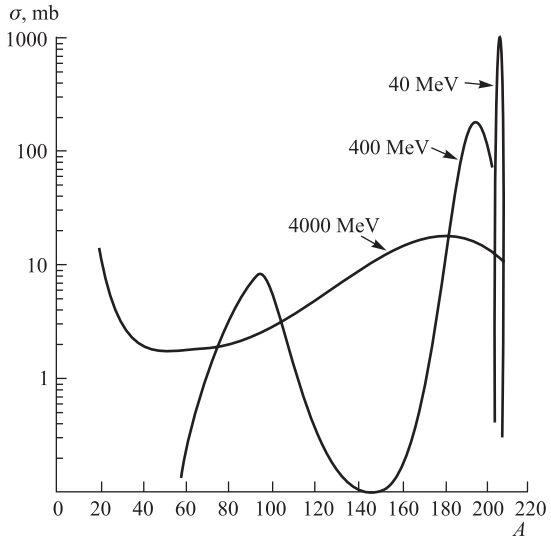

Fig. 10. A textbook figure showing the mass distributions of products formed in thin Bi targets and irradiated with 40, 400, and 4000 MeV protons. (This picture is taken from [12].) Similar results have been found for thin Cu targets

it is shown that low-energy protons produce predominantly spallation products close to the target nucleus. Surprisingly, the secondary fragments produced in our experiment with 72 GeV ^{40}Ar do not produce any enhancement in the second Cu disk of masses close to the target mass as one would have expected for low-energy secondary particles, and as it is also demonstrated in Table 1. For the mass $A = 59$, the experimental ratio $B(A)_{\rm second}/B(A)_{\rm prim}$ is about 1.8 both for the 3 GeV ^2d irradiations as well as for 72 GeV ^{40}Ar irradiations, despite the fact, that in the low-energy irradiation less than 1 hadron is emitted as a secondary fragment and in the high-energy irradiation about 23 hadrons are emitted with $E > 50$ MeV as secondaries. It appears that the majority of all secondary p, n, and π produced by 72 GeV ^{40}Ar behave almost like primary particles in the GeV-energy range. This is still another aspect of unresolved problems observed with radiochemical techniques in thick Cu targets. It is impossible to decide with the very crude «two-Cu-disks» experiment if all secondary fragments behave the same, or if some of them interact just «normal» and some others interact «not normal». This problem will be considered further in one of the following sections.

The early Cu-disk experiments in Berkeley did not only include irradiations of two Cu disks, but also one irradiation of a compact 20 Cu-disks target with 72 GeV ^{40}Ar. This latter target was irradiated in 1987 for 44 min with a total fluence of $1.2 \cdot 10^{12}$ ions [24]. During this irradiation one observed surprisingly large and unexpected neutron fluences, even outside the immediate experimental area, as has been reported by Wang [25]: «In 1987, [a scientist] and his colleagues were irradiating their samples at the relativistic heavy ion accelerator Bevalac at Lawrence Berkeley Laboratory (LBL), USA. It was discovered that great amounts of fast neutrons were produced in the target area and spread in the accelerator hall, which constituted considerable radiation hazards to scientists and operators working near the high-energy accelerator. Later, when [a scientist] and his colleagues went to the Joint Institute for Nuclear Research (JINR), Dubna, Russia, to make a higher energy heavy-ion experiment, they deployed [various techniques] and further proved that copious amounts of fast neutrons are produced in relativistic heavy-ion interactions». No quantitative results of neutron measurements in the Berkeley experiment have been published. After the irradiation in Berkeley, only the induced radioactivity was measured in several Cu disks and analyzed in a usual way. Earlier presentations in this paper considered global aspects in the irradiation of 20 cm Cu targets in Dubna as shown in Fig. 3. Now we will concentrate on the investigation of selected product yields in specific Cu disks of the 20 cm stack. In Fig. 11, the results are shown for a few isotopes comparing the irradiations with 72 GeV ^{40}Ar in Berkeley and with 3 GeV deuterium in Dubna. The 3 GeV deuterium results are well understood in a conventional manner. There is a large production of ^{57}Ni isotopes in all Cu disks showing a strong increase within the first 8 cm of the Cu target, less production of ^{44}Sc and

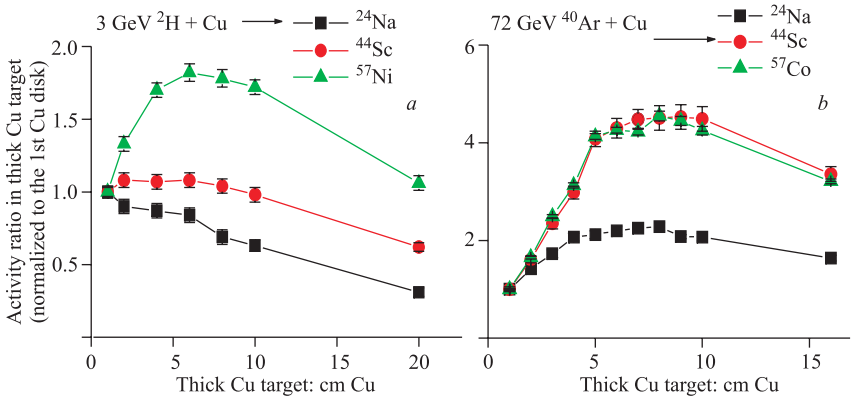

Fig. 11. Cross-section ratios for specific isotopes within the 20 cm Cu target, normalized to the first Cu disk for two irradiations with 3 GeV deuterium (*a*) in Dubna and 72 GeV ^{40}Ar (*b*) in Berkeley. For details see the text

a steady and almost linear decrease of the ^{24}Na activity when going downstream through the Cu target. In the irradiation with 72 GeV ^{40}Ar, this being a beam with high total energy, one observes a distinctly different pattern which strongly resembles the irradiation with 44 GeV ^{12}C. Activities of ^{57}Co, ^{44}Sc, and ^{24}Na increase within the first 6 to 10 cm of the target and then afterwards they decrease slowly. There is no difference observed in the ^{44}Sc and ^{57}Co activity distribution despite the fact that their production from Cu has distinctly different threshold energies (see Fig. 9). This is a qualitative description of the observed findings.

A quantitative interpretation for the production of ^{24}Na in the 20 cm copper experiment with 72 GeV ^{40}Ar was given by L. Lerman [2]. Following a suggestion by E. M. Friedlander (Brandt R. Private communication. 1985), Lerman irradiated a nuclear emulsion target with 72 GeV ^{40}Ar ions and analyzed the nuclear tracks under an optical microscope with the help of an experienced team of scanners in Bucharest (Leader: M. Haiduc). They determined all properties, such as track length before the first interaction, track length and nuclear charges of projectile fragments ($Z > 1$) between the first and possibly the second nuclear interaction, etc. Lerman used these data as input data for Monte Carlo calcula-

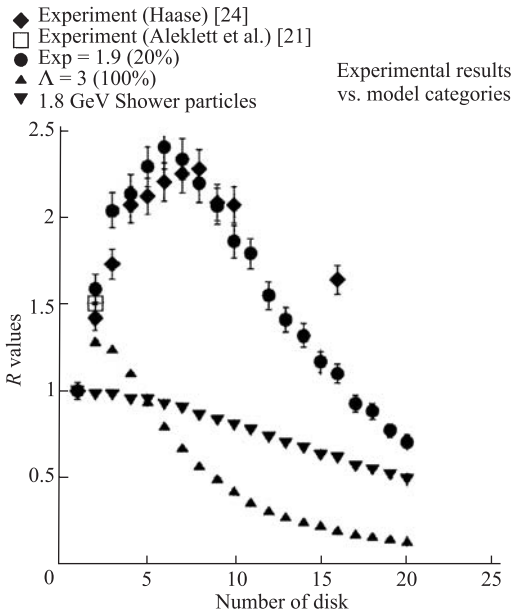

Fig. 12. The distribution of $R_i(^{24}\text{Na})$ within compact 20 Cu disks (1.0 cm thickness) in the irradiation with 72 GeV ^{40}Ar ions in Berkeley. $R_i(^{24}\text{Na})$ is the relative ^{24}Na activity in the ith Cu disk as compared to the first disk. The experimental results are given together with model calculations, explained in the text. The graph is from Lerman [2]

tions of the ^{24}Na production in Cu taking into account the well-known excitation function for the production of this isotope from Cu [20, 21]. The comparisons of experimental cross-section ratios $R_i(^{24}\mathrm{Na})$ with a variety of theoretical model calculations are shown in Fig. 12.

• Assuming that all secondary «shower particles» ($Z = 1$, $E > 400$ MeV) have the extreme primary kinetic energy of 1.8 GeV/A ($72 : 40 = 1.8$) and all heavy secondary projectile fragments behave just as expected from known physics, the results of the simulating calculation show a slow decrease of the ^{24}Na activity with increasing depth into the Cu target. Thus, the most reasonable input parameters for the calculation give poor agreement with the experimental observations.

• Alternatively, one can assume that all heavy secondary projectile fragments with $Z > 1$ and mass A_p have a reduced mean free path $\Lambda(A_p) > 8$ cm [2]. Then the calculation gives a slight increase for the ^{24}Na activity in the second and third Cu disks. However, this increase is followed by a very drastic decrease of the ^{24}Na activity in the following disks. Again, the agreement between experiment and model calculation is poor. The assumption of a reduced mean free path is based on the «anomalon hypothesis» as suggested by Friedlander et al. [16] and reviewed by Ganssauge [17]. More precisely, this assumption is considered as a part of the «physical anomalon» hypothesis which has been introduced by Dutta et al. [18]. Aleklett et al. [21] had also suggested the same hypothesis for the interpretation of the enhanced production of ^{24}Na in the second Cu disk. In view of Lerman's analysis this interpretation may now be considered as being incorrect.

• One may assume *ad hoc* an «enhanced production cross section» for ^{24}Na in Cu for, e.g., 20% of all projectile fragments ($Z > 1$) by scaling with $\sigma(A_p)_{\mathrm{ad\,hoc}} = 3.6A_p^{1.9}$ in contrast to the normal scaling relation $\sigma(A_p)_{\mathrm{normal}} = 3.6A_p^{0.387}$ (for details see [2]). This means practically a factor of about 32 for projectile fragments with a selected mass $A_p = 10$:

$$\frac{\sigma(A_p = 10)_{\mathrm{ad\,hoc}}}{\sigma(A_p = 10)_{\mathrm{normal}}} = \frac{A_p^{1.9}}{A_p^{0.387}} = 32. \tag{3}$$

• Using this procedure, one can observe a nearly perfect agreement between experiment and model calculation. In this case, the model calculation correctly describes the enhancement of the ^{24}Na production in dowstream Cu disks within the first 8 cm, followed by the expected decrease even further downstream. This «enhancement factor» of 32 for a specific projectile fragment A_p can be compared with a similar «enhancement factor» of 3.4 for all secondary products ($1 \leqslant A_p \leqslant 65$), including protons and neutrons, as employed in a related analysis [1]. Again, the *ad hoc* assumption is based on the «anomalon hypothesis» mentioned already. More precisely, this assumption is considered as a part of the «chemical anomalon

hypothesis» as it has been introduced by Dutta et al. [18]. The physical relevance of such a hypothesis remains to be elaborated as this constitutes a further aspect of unresolved problems.

This section on radiochemical evidence in thick and compact targets shall be terminated with a look at further experiments with other techniques confirming (or not) the conclusions of this section.

Secondary fragments produced in the interaction of heavy ions with a total energy E above 10 GeV seem to excite (i.e., destroy) target nuclei stronger than their primary heavy parent ions. This effect has been measured in copper targets irradiated with 44 GeV ^{12}C from Dubna and 72 GeV ^{40}Ar from Berkeley. The reason for this behavior is presently unknown. The phenomenon constitutes one of the unresolved problems described in this paper. These observations may have consequences that require consideration: Secondary fragments produce in copper targets more products with a large mass difference ΔA from the target than the primary heavy ion does. In addition, the abundant production of secondary protons, neutrons, and pions with energies below 300 MeV is not reflected in the production of abundant spallation products with small ΔA from the target. The open question is: Where did the lost masses end up, when such a shift to lower target-like masses is observed experimentally? One can speculate that these lost masses may have been emitted as single neutrons and/or protons from the thick target. Indeed, Vassilkov et al. [10] have published as early as 1983 an experimental observation of such an «enhanced neutron production» in thick lead targets during the irradiation with 44 GeV ^{12}C. This will be discussed in the next section. It is a strange fact, not at all unique in science though, that this surprising enhanced neutron production has been observed a long time before anybody was thinking about the radiochemical observations described here for thick Cu targets and nobody seemed to care. In the following sections we will investigate the corresponding wide-angle emission ($\Theta > 11^\circ$) of secondary hadrons and the evaporation of protons (studied as «black prongs» in nuclear interactions induced by high energy heavy ions in nuclear emulsions). In the end one can arrive at a description of possible consequences of these new findings [12, 26].

3. NEUTRON EMISSION FROM THICK AND COMPACT Cu AND Pb TARGETS

The study of the neutron emission in interactions of relativistic projectiles using different target systems has a long tradition. Vassilkov and co-workers have studied the neutron emission of extended lead targets irradiated with many heavy ions available at the Synchrophasotron accelerator in Dubna using specific energies E/A in the range from 1 GeV/A up to the maximum of 3.7 GeV/A. Their experiments were carried out as early as in 1980 [10]. The lead target

employed in their investigations had dimensions of 20 cm diameter and a length of 60 cm and it was placed inside a large 1 m^3 paraffin block to allow for neutron moderation. The number of thermal neutrons n per incoming relativistic heavy ion was measured using advanced detection systems of their time. Their experimental results are presented in Figs. 12, 13, and in Table 2.

Table 2. **The total number of thermal neutrons n, generated by one primary ion (^{1}H, ^{2}H, ^{4}He, or ^{12}C) in a lead target [10] as shown in Figs. 12 and 13. The last column gives the ratio of the neutron yield at the specific energy $E/A = 3.7$ GeV/A as compared to $E/A = 1.0$ GeV/A for all the four beam ions investigated. Further details are given in the text**

Ion	Mass A	Thermal neutrons n		$\frac{n \text{ at } (E/A = 3.7 \text{ GeV}/A)}{n \text{ at } (E/A = 1.0 \text{ GeV}/A)}$
		at $E/A = 1$ GeV/A	at $E/A = 3.7$ GeV/A	
P	1	16.5 ± 0.5	49.4 ± 1.9	**3.0 ± 0.2**
H	2	45.8 ± 1.2	157 ± 3	3.4 ± 0.2
α	4	71.2 ± 2.8	277 ± 9	3.9 ± 0.2
C	12	129 ± 5	641 ± 22	**5.0 ± 0.3**

The relative neutron production rate $R(n/E)$ for thermal neutrons per ^{1}H, ^{2}H, ^{4}He, and ^{12}C ion is shown in Fig. 14 in the range of the specific ion energy, E/A, between 1.0 and 3.7 GeV/A. $R(n/E)$ is the total number of neutrons produced, divided by the total kinetic energy E of the projectile in GeV. A nearly

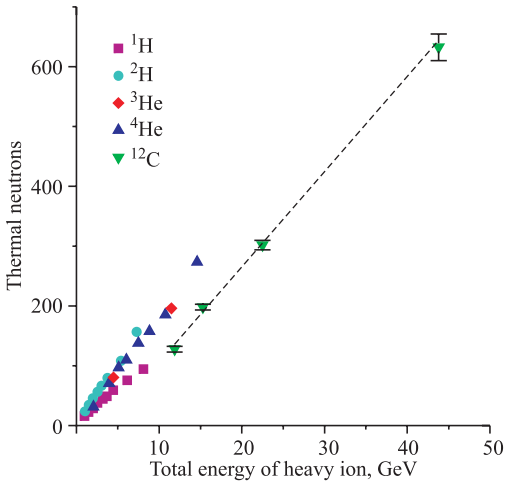

Fig. 13. The number of thermal neutrons n per primary ion in a Pb target placed inside a 1 m^3 paraffin moderator was measured by Vassilkov et al. [10]. The irradiations were carried out at the Synchrophasotron in Dubna. Only the experimental points for the ^{12}C irradiation are connected by a line in order to guide the eye. There are no experimental results reported for energies $E(^{12}\text{C}) < 12$ GeV. Further details are given in the text

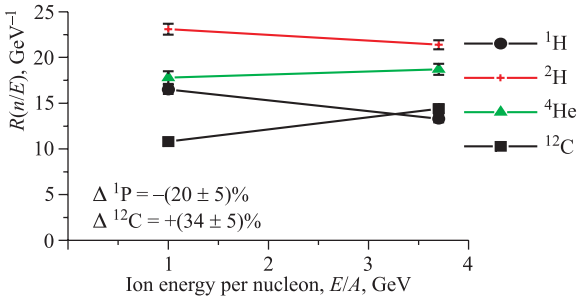

Fig. 14. The relative production rates $R(n/E)$ of thermal neutrons per ^{1}H, ^{2}H, ^{4}He, or ^{12}C ion between two specific energies $E/A = 1.0$ GeV/A and $E/A = 3.7$ GeV/A using the results shown in Fig. 12. The values $\Delta(^1\mathrm{H})$ and $\Delta(^{12}\mathrm{C})$ are the change in $R(n/E)$, when E/A increases from 1.0 to 3.7 GeV/A for ^{1}H and ^{12}C, respectively [10]

constant relative production rate $R(n/E)$ of thermal neutrons n with increasing bombarding energy E is observed for all irradiations. However, when looking in more detail into the numbers, one finds a slight decrease in $R(n/E)$ for protons, measured as $\Delta(^1\mathrm{H})$ which is defined as follows:

$$\Delta(^1H) = \frac{R(n/E)_{[3.7\,\mathrm{GeV\ prot.}]} - R(n/E)_{[1\,\mathrm{GeV\ prot.}]}}{R(n/E)_{[1\,\mathrm{GeV\ prot.}]}}. \tag{4}$$

The results stated in Table 2 and in Fig. 13 give $\Delta(^1H) = -(20 \pm 5)\%$ when the proton energy increases from 1 to 3.7 GeV. This decrease is in qualitative agreement with theoretical calculations [27, 28]. The results for ^{2}H, ^{4}He, and ^{12}C ions are found in an analogous manner. However, for ^{12}C irradiations one observes experimentally just the opposite trend as compared to protons:

$$\text{for } 12 \text{ GeV}^{12}\mathrm{C}\left(\text{or}\,\frac{E}{A} = 1.0 \text{ GeV}\right) : R\left(\frac{n}{E}\right)_{12\ \mathrm{GeV}\ ^{12}\mathrm{C}} = (10.8 \pm 0.4)\ \mathrm{GeV}^{-1},$$

$$\text{for } 44 \text{ GeV}^{12}\mathrm{C}\left(\text{or}\,\frac{E}{A} = 3.7 \text{ GeV}\right) : R\left(\frac{n}{E}\right)_{44\ \mathrm{GeV}\ ^{12}\mathrm{C}} = (14.5 \pm 0.5)\ \mathrm{GeV}^{-1}.$$

In the ^{12}C case, one finds an increase in $R(n/E)_{^{12}\mathrm{C}}$ with rising energy of the ^{12}C ions, yielding $\Delta(^{12}\mathrm{C}) = +(34 \pm 5)\%$. This experimental result is statistically quite significant, however, there is no theoretical concept available to understand this observation [27, 28]. The same deficiency had already been noticed by Vassilkov et al. [10] and it must be considered as another unresolved problem in this paper. It is apparently another aspect of phenomena described earlier in connection with the excessive ability of secondary fragments produced by 44 GeV ^{12}C in thick Cu targets to deposit energy in target nuclei. It should

be repeated that these effects have been described in [27] as [quote] «obeying from a fundamental point of view a logic of $(1 + 1 = 3)$». Other interpretations could also be possible. However, in combination with the radiochemical yield observations in thick targets irradiated with 44 GeV ^{12}C, no other interpretation appears to be consistent with all known experimental observations. Potential practical applications of this observation will be mentioned in Conclusion.

A particularly significant aspect is given in the last column of Table 2. The ratio $\{(n$ at $[E/A = 3.7$ GeV/$A])/(n$ at $[E/A = 1.0$ GeV/$A])\}$ gives the ratio of the neutron yield at 3.7 GeV/A divided by the yield at 1.0 GeV/A. This ratio 3.0 ± 0.2 for protons is in good agreement with theoretical estimates [27, 28]. However, with heavier projectiles this ratio increases up to the value of 5.0 ± 0.3 for ^{12}C ions, which is again completely outside of results from any theoretical model in nuclear physics, as known to the authors: this increase in neutron yield by the value of 5.0 ± 0.3 is significantly stronger than the increase in the input energy by a factor of 3.7.

Similar effects have also been observed in other experiments. Tolstov (JINR, Dubna) described experiments using a massive Pb block ($0.5 \times 0.5 \times 0.8$ m) in irradiations with the same set of relativistic ions as employed by Vassilkov (*loc. cit.*). Tolstov studied the production of secondary neutrons by measurement of the transmutation rate ^{238}U into ^{239}Np, as given in the equation

$$^{238}\mathrm{U} + n \rightarrow {}^{239}\mathrm{U} \rightarrow {}^{239}\mathrm{Np}\,(\mathrm{radioactive}). \tag{5}$$

Results for proton, deuteron, and alpha-particle irradiations were quite compatible with his model calculations. However, in the irradiation with 44 GeV ^{12}C he obtained transmutation yields for ^{239}Np that were about a factor of two larger than predicted by the same model calculations. This experiment is described and referenced in detail in [27].

Another systematic study of total neutron production was carried out by Ochs et al. [28] using 8 cm diameter and 20 cm long Cu or Pb targets surrounded by a 6 cm paraffin moderator as shown in Fig. 15.

The irradiations were carried out at the Synchrophasotron using the same projectiles as Vassilkov (*loc. cit.*) but with a target and moderator in smaller dimensions. Two neutron capture reactions ($^{238}\mathrm{U} \rightarrow {}^{239}\mathrm{Np}$ and $^{139}\mathrm{La} \rightarrow {}^{140}\mathrm{La}$) were used as sensors for neutron fluence determinations by measuring the decay of the radioactive reaction products given in equations (4) and (5)

$$^{139}\mathrm{La} + n \rightarrow {}^{140}\mathrm{La}\,(\mathrm{radioactive}). \tag{6}$$

The La and U sensors with weights of approximately 1 g each were placed on the top of the moderator in positions (1–5). In addition, more La sensors were positioned at locations (6–12) around the moderator in order to estimate the azimuthal distribution of the neutron fluence. The effects of an asymmetric neutron

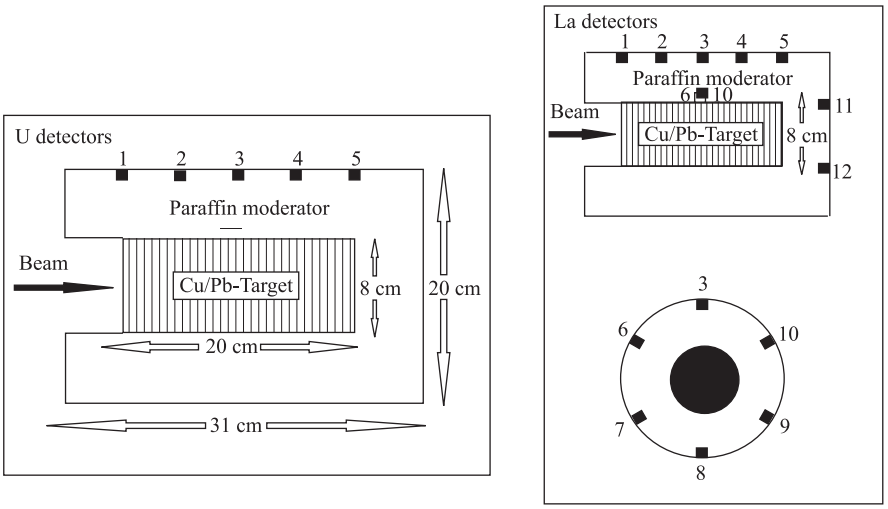

Fig. 15. Experiments using extended Cu or Pb targets for the production of secondary neutrons with heavy ions. The target is surrounded by paraffin to moderate these secondary neutrons [28]. For details see text

distribution could be corrected for [28]. The resulting B-value distributions (the parameter B has been defined before, see Eq. (1)) are given as the average of B values in positions (1–5) and presented in Fig. 16. Again, one can observe a qualitatively similar, but not identical behaviour as also seen by Vassilkov and Tolstov. Reactions induced by 44 GeV ^{12}C ions show a considerably stronger increase of energy in yields for nuclear reactions as compared to lower energy reactions induced by deuteron and alpha beams. However, it is obvious that the results from the Vassilkov group are most significant, both from the point of view of priority as well as from statistical significance.

Apparently, the measured effects of a more-than-expected increase in neutron production and the related increase in transmutation yields is connected with 44 GeV ^{12}C irradiations of thick Cu and Pb targets. A similar finding was reported for the 72 GeV ^{40}Ar irradiation in Berkeley by Wang [25]. However, no quantitative results had been published about the observation in Berkeley. The above-mentioned rather fragmentary observations of a more-than-linear increase of neutron production when the total projectile energy exceeds some limit value do not allow any systematic analysis.

On the other hand, one had carried out systematic studies with a variety of relativistic ions on the two-Cu-disks configuration using radiochemical methods, as already described in Sec. 2. Detailed results for the $R_0^{\exp}(^{24}\mathrm{Na})$ distributions

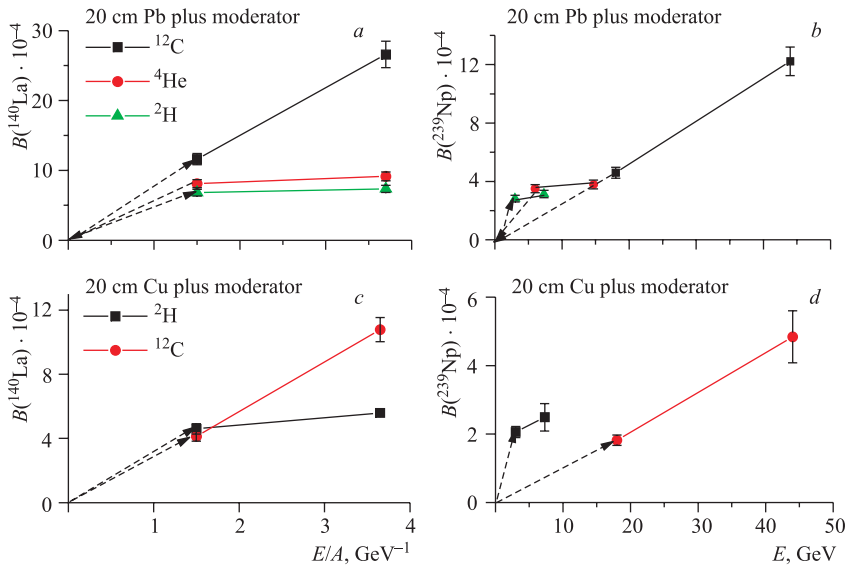

Fig. 16. Transmutation yields B using 20 cm long Pb or Cu targets plus 6 cm paraffin moderators (see Fig. 15) and irradiated in Dubna with ^{2}H, ^{4}He, and ^{12}C ions. The neutron fluence per ion was measured with La and U sensors on the top of the moderator using (n, γ) reactions [28]. Details are described in the text

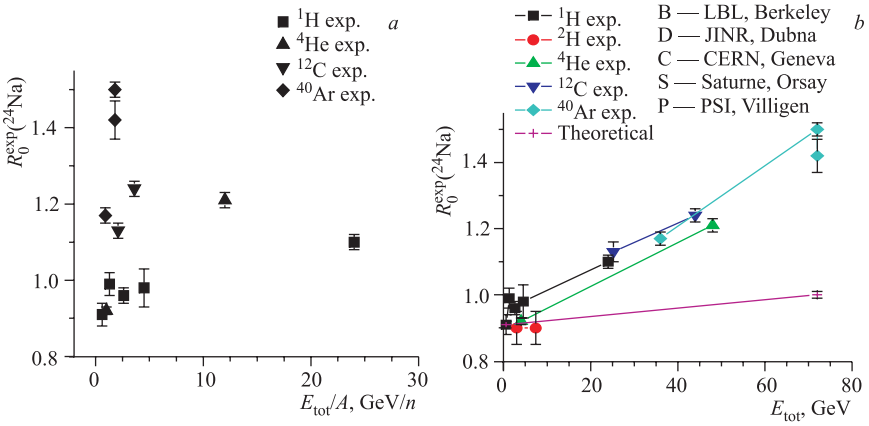

Fig. 17. *b*) The observed linear increase in $R_0^{\mathrm{exp}}(^{24}\mathrm{Na})$ with the total energy, E, of the projectile. The «theoretical» line is given to guide the eye [1]. *a*) No similar correlation between $R_0^{\mathrm{exp}}(^{24}\mathrm{Na})$ and the specific projectile energy, E/A, can be observed [2]

in these two-Cu-disks experiments within a broad range of various ions in the energy range from 0.6 to 72 GeV total energy, E, are available. Therefore, we

can present in Fig. 17, a a plot of the $R_0^{\exp}(^{24}\mathrm{Na})$ distributions as a function of the specific energy E/A. An analogous representation of the same R_0 values as a function of the total energy, E, is shown in Fig. 17, b. There is no correlation between the two parameters in Fig. 17, a, but there is a nice linear correlation between $R_0^{\exp}(^{24}\mathrm{Na})$ and the total energy, E_{tot}, in Fig. 17, b. The «theoretical» value for $R_0(^{24}\mathrm{Na})$ at 72 GeV is also included as described in Sec. 2 [1, 2]. The value $R_0^{\exp}(^{24}\mathrm{Na})$ at 0.6 GeV agrees with model calculations [1] and the line labelled «theoretical» between these two points is drawn to guide the eye. The authors are not aware of any model calculations that will reproduce this experimental observation.

It has been described that «excess neutrons» are produced by secondary fragments in thick targets for total energies E above 30 GeV. In the next section we will describe the investigation of the number of «black prongs» observed in nuclear emulsions in the first and consecutive second nuclear interactions along the path of relativistic high-energy heavy ions, in this study for 72 GeV ^{22}Ne.

4. EVAPORATED PROTONS («BLACK PRONGS») DUE TO NUCLEAR INTERACTIONS OF 72 GeV ^{22}Ne IN NUCLEAR EMULSIONS

In the early part of this paper some radiochemical experiments were described, which will be shortly recapitulated in order to explain the rationale of this section: The mass-yield curve of 3 GeV deuterium in a thick Cu target is rather «normal» as shown in Figs. 3 and 4; there are many spallation products close to ^{63,65}Cu such as ^{59}Fe, less ^{43}K and very little yield of ^{24}Na. This yield curve is within the concept of «limiting fragmentation» and the same holds also for the 44 GeV ^{12}C irradiation of a thin Cu target (see Fig. 1). However, the observed mass-yield curve in a thick Cu target induced by 44 GeV ^{12}C shows only a small ^{59}Fe yield, plenty of ^{43}K and an enhanced yield of ^{24}Na due to secondary fragments (see Fig. 3). This demonstrates directly that secondary fragments excite copper nuclei much stronger than primary ions like 44 GeV ^{12}C. Such phenomena have been observed in radiochemical investigations.

The same findings should also be expected in nuclear emulsions irradiated with relativistic heavy ions of about the same total energy. It has been pointed out in earlier publications [20, 21] that nuclear emulsions and copper behave in a rather similar fashion in interactions with heavy ions. As there is evidence that secondary fragments induce stronger nuclear excitation than primary ions, it will be the aim of this section to compare the nuclear excitation induced in the first nuclear interaction in nuclear emulsions with the excitation induced in the consecutive second nuclear interaction of a relativistic heavy secondary fragments along the path of one heavy ion track.

A typical example for such an investigation is the trail of a single 100 GeV ^{56}Fe track in nuclear emulsion shown in Fig. 18 [29]. Four nuclear interactions are observed during the passage of this relativistic ion through 5.7 cm of nuclear emulsion material. Each interaction is characterized by an observable «star» with several different types of reaction products.

• The original 100 GeV ^{56}Fe ion moves straightforward as heavily ionizing particle, leaving a track in the nuclear emulsion.

• The so-called «minimum ionizing particles» produce very thin tracks. They are predominantly moving in the forward direction and are relativistic protons with energies above 400 MeV or pions above 56 MeV. In this «first-order aproximation» study we have neglected these particles, although it is clear that also these particles have significant cross sections for nuclear interactions in copper (see the next section). Consequently, the conclusion of this section can have only a validity within the restrictions given.

• The so-called «black prongs» are produced most-of-the-time by heavily ionizing protons with energy below 30 MeV. They are easily recognized as they are emitted isotropically into all lab angles. This is due to the fact that they are emitted from an excited target-like nucleus at rest in the lab system. The number of «black prongs» in one interaction is denoted with the symbol N_b. It is a measure for the excitation of the target nucleus.

• The so-called «grey prongs» are $Z = 1$ particles with proton energies between ($30 < E_p < 400$ MeV). The sum of «black prongs» and «grey prongs» is called «heavy prongs», denoted as N_h and introduced in Sec. 1.

It is the aim of this study to compare $\langle {}^1N_b \rangle$, i.e., the average number of «black prongs» in the first nuclear interactions of the primary ion, with $\langle {}^2N_b \rangle$, the average number of «black prongs» in the second nuclear interactions of the projectile-like secondary fragment. We choose in this survey to study nuclear interactions along tracks of 72 GeV ^{22}Ne ions in a nuclear emulsion stack which had been irradiated many decades ago. The aim of this study was to answer the question: *Is the average number $\langle {}^1N_b \rangle$ in the first nuclear interaction significantly different from the average number $\langle {}^2N_b \rangle$ in the second nuclear interaction for 72 GeV ^{22}Ne ion tracks in nuclear emulsions?*

Therefore we concentrated on those tracks from 72 GeV ^{22}Ne in nuclear emulsion, where the first nuclear interaction could be observed and at least one relativistic heavy, ($Z > 1$), secondary fragment was produced in this interaction. Altogether, 164 events of this type could be registered in this class. The relativistic heavy, ($Z > 1$), secondary fragments were followed within the nuclear emulsion and in 71 cases the second nuclear interactions could be observed. The other 93 events did not have an observable second nuclear interaction within the limited geometry of the nuclear emulsion used. These 71 interactions are important for the present study, they are of a type as indicated schematically in Fig. 6, c with the signature «Ar-3». These interactions can be responsible for any «enhancement

effects» due to relativistic secondary fragments in the two-Cu-disks experiments described earlier in Sec. 2. The other types of interactions, denoted as «Ar-1» and «Ar-2» in Fig. 6, *c*, can be ignored in our specific study.

First results have been published elsewhere [13] and will be quoted here. The total of 230 observed first nuclear interactions gave an average number of black prongs per event:

$$\langle {}^1N_b\rangle_{\text{all interac}} = 6.60 \pm 0.17(\pm 0.15). \tag{7}$$

The statistical uncertainty is given first, followed by another uncertainty in parentheses which is due to technical difficulties in the differentiation between black prongs ($E_p < 30$ MeV) and grey prongs ($30 < E_p < 400$ MeV). This result in Eq. (7) includes all interactions, i.e., those with no further relativistic heavy, ($Z > 1$), fragments (66 events) and those where at least one further heavy, ($Z > 1$), secondary fragment (164 events) was produced.

Selecting out of the 230 first interactions only those with at least one relativistic heavy, ($Z > 1$), secondary fragment (164 events), one finds an average number of black prongs per event, $\langle N_b^1\rangle_{\text{sel}}$:

$$\langle {}^1N_b\rangle_{\text{sel}} = 4.57 \pm 0.17(\pm 0.10). \tag{8}$$

The average number of black prongs per event, $\langle {}^2N_b\rangle$, in all the second nuclear interactions induced by relativistic heavy, ($Z > 1$), secondary fragments was found for 71 interactions as:

$$\langle {}^2N_b\rangle = 7.42 \pm 0.32(\pm 0.28). \tag{9}$$

Here, all interactions have been included, i.e., those producing and those not producing further heavy, ($Z > 1$), third generation fragments. The ratio ($\langle {}^2N_b\rangle/\langle {}^1N_b\rangle_{\text{sel}}$) can be calculated again with a statistical uncertainty given first, followed by another uncertainty in parentheses which is due to technical difficulties in the differentiation between black prongs ($E_p < 30$ MeV) and grey prongs ($30 < E_p < 400$ MeV):

$$\frac{\langle {}^2N_b\rangle}{\langle {}^1N_b\rangle_{\text{sel}}} = 1.63 \pm 0.09(\pm 0.07). \tag{10}$$

This increase above unity by $(63 \pm 16)\%$ is statistically significant and may confirm independently the enhanced ability of relativistic heavy, ($Z > 1$), secondary fragments to excite target nuclei stronger as compared to the primary beam particle. However, this conclusion must not necessarily be correct, as we have in the parameter $\langle {}^1N_b\rangle_{\text{sel}}$ a somewhat arbitrary selection of the first nuclear

interactions of the beam ion. When one compares $\langle {}^2N_b\rangle$ with $\langle {}^1N_b\rangle$ for all the first nuclear interactions one obtains with the same uncertainties as above:

$$\frac{\langle {}^2N_b\rangle}{\langle {}^1N_b\rangle_{\text{all interac}}} = 1.12 \pm 0.06(\pm 0.05). \tag{11}$$

This ratio does not show a statistically significant difference from unity and consequently does not support the result of Eq. (10). As this study of the second nuclear interactions (in other words: in thick targets) is the first of its kind known to the authors, one needs further studies to confirm (or not confirm) the physical significance of all these results. In particular, further emulsion studies appear to be desirable. In addition, investigations of nuclear interactions induced by ($Z \leqslant 1$)-secondary projectile fragments (protons, neutrons, pions) should be carried out by several independent methods, such as we do in the next section using radiochemistry methods.

Finally, it appears to be useful to discuss two further related aspects of these emulsion experiments.

It is recalled that in emulsion studies one often discriminates between two classes of events that differ in the number of «heavy prongs», N_h, where heavy prongs are the sum of black prongs and grey prongs [2, 21]. These studies have been restricted to the first nuclear interaction of the projectile in the nuclear emulsion plate and a separation of events is made between $N_h \leqslant 8$ and $N_h > 8$. In Fig. 2 above, the universal validity of «integral frequency distributions», $F(\geqslant N_h)$, is demonstrated. The shape of the distributions is independent of the proton energy E_p, provided that E_p exceeds 1 GeV. It can be concluded from this universal validity that the ratio of the number of events with $N_h \leqslant 8$ compared to the number of events with $N_h > 8$ is independent of the energy of relativistic protons. This principle will be tested in this work with respect to the behaviour of the second nuclear interaction as compared to the first nuclear interaction.

«Black prong» multiplicities, N_b, for the second and first nuclear interactions are studied and we introduce *ad hoc* and without any claim of a physical significance a separation of events into classes by two different separation values:

• A separation of events into two classes is carried out between $N_b \leqslant 4$ and $N_b > 4$. The choice of this value 4 is purely practical, not based on serious scientific arguments, as the total number of events studied here is rather limited and any other separation would give statistically less significant results. The universal validity of integral frequency distributions, $F(\geqslant N_h)$ in Fig. 2, can be tested with any separation line.

• Another separation of events into two classes is carried out between $N_b \leqslant 12$ and $N_b > 12$. The resulting multiplicities are shown in Table 3. Due to the small number of total events, any subdivision into classes results in a lower number of events and statistics deteriorate. However, the ratio of events in the second compared to the first nuclear interactions appears to increase with increasing

Table 3. **Results of nuclear emulsion studies for interactions by 72 GeV ^{22}Ne. The number of events is given together with their observed mean value of «black prongs», $\langle N_b \rangle$, for the first and second nuclear interactions**

Line	Event class	First interactions where relativistic fragments with $Z > 1$ are produced	All second interactions	Ratios between number of events and between mean black prongs in the second and in the first interactions
1a	All events	164 (100%) events	71 (100%) events	0.45
1b	$\langle N_b \rangle$	**4.57 ± 0.17 (± 0.10)**	**7.42 ± 0.32 (± 0.28)**	**1.63 ± 0.09 (± 0.07)**
2a	Events with $N_b \leqslant 4$	103 (63%) events	35 (49%) events	0.34
2b	$\langle N_b \rangle$	1.53	1.813	1.2
3a	Events with $N_b > 4$	61 (37%) events	36 (51%) events	0.59
3b	$\langle N_b \rangle$	9.7	12.9	1.33
4a	Events with $N_b > 12$	17 (10%) events	18 (25%) events	1.06
4b	$\langle N_b \rangle$	16	18	1.12

threshold for N_b, though this increase is not yet statistically significant. One cannot assign a significant uncertainty to these ratios. Consequently, one must wait with any conclusion in this respect until results from more measurements of nuclear interactions in nuclear emulsions are available. Further details are given in [13].

In Fig. 18 one observes the complete destruction of a target nucleus at the end of the passage through the nuclear emulsion of a 100 GeV ^{56}Fe ion. Such an effect has occasionally been observed and evidences have been summarized by Tolstov [30]. Ganssauge showed in a review one example observed in nuclear emulsions of the complete destruction of a 228 GeV ^{238}U projectile at the end of its path [17]. Many similar complete evaporations of 228 GeV ^{238}U projectiles have been observed in a thick CR-39 solid state nuclear track detector (SSNTD) stack after irradiations at the Bevalac accelerator in Berkeley [31]. However, no such destruction could be observed in the same CR-39 set-up irradiated with 109 GeV ^{238}U ions [31]. These observations of effects in CR-39 have not yet been experimentally confirmed.

As has been mentioned already, one event class has not been considered properly: First nuclear interactions induced by a primary ^{22}Ne ion and resulting in zero projectile fragments with $Z > 1$ could not be followed into their second nuclear interaction. In these interactions only «minimum ionizing particles» were observed. Secondary nuclear reactions induced by these «minimum ionizing par-

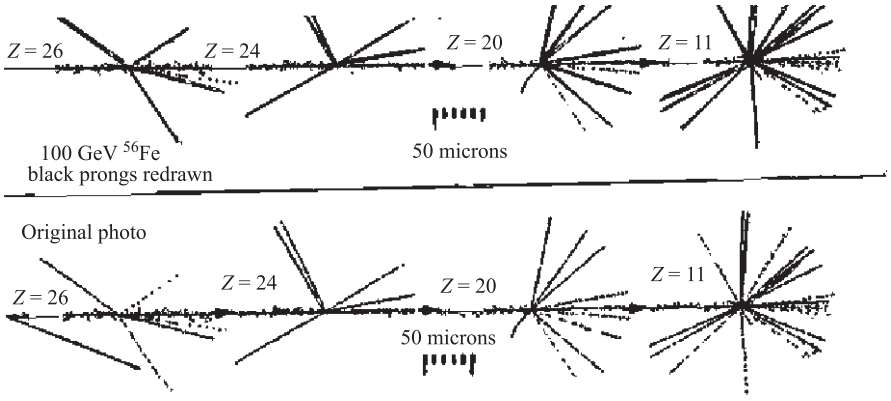

Fig. 18. A sequence of four fragmentation reactions initiated successively in nuclear emulsion by a single 100-GeV ^{56}Fe ($Z = 26$) ion that enters from the left (Friedlander, Heckmann. 1983) [29]. The actual distance between beam entrance into the emulsion and the final interaction is 5.7 cm

ticles» could not be investigated simply for technical reasons within the emulsion plate employed as they are emitted into wide forward angles and thus easily escape this very thin emulsion plate. In the next section radiochemical studies of secondary ($Z \leqslant 1$) particles, including «minimum ionizing particles» emitted into large lab angles of $\Theta > 11^\circ$ will be presented.

5. INTERACTIONS OF WIDE-ANGLE ($\Theta > 11^\circ$) EMITTED SECONDARY ($Z \leqslant 1$) PARTICLES

5.1. Studies on the Production of the Isotope ^{24}Na in the Diluted «2π-Cu Target». The Cu-disks experiments studied so far in this paper gave some evidence for enhanced nuclear excitation induced by secondary fragments in the forward beam direction. Detailed information on any angular dependence (if any) of this effect is rather fragmentary. Comparing $R_0(^AZ)$ with $R_{20}(^AZ)$ for two Cu disks irradiated with 72 GeV ^{40}Ar (see Fig. 6) one observes a considerably smaller contribution of secondary fragments to the production of radioactive nuclides in the second Cu disk at a 20 cm distance (measured as $R_{20}(^AZ)$) as compared to a 0 cm distance (measured as $R_0(^AZ)$). This is due to the restricted registration efficiency of $\Theta < 10^\circ$ for secondary fragments in the second Cu disk in a 20 cm distance downstream. The problem of the «lost radioactivity» was studied with the more complex experimental set-up, called «2π-Cu target» shown in Fig. 19 [4]. This arrangement consisted of two Cu disks ($\varnothing = 8$ cm, $d = 1$ cm) separated by 20 cm, where the downstream disk subtends an angle of $\Theta < 10^\circ$.

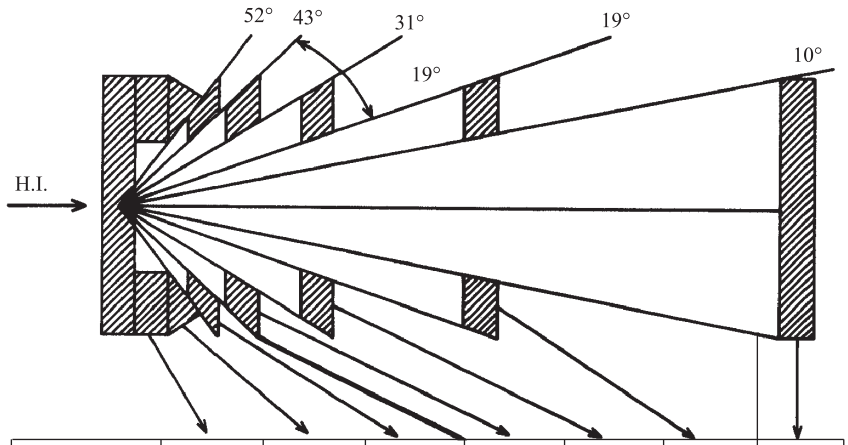

R (^{24}Na), °	90–70	70–52	52–43	43–31	31–19	19–10	10–0
4 GeV ^{4}He Saturne (France), %	0.2±0.1	0.1±0.1	0.2±0.1	0.3±0.1	0.5±0.1	0.8±0.1	90±1
44 GeV ^{12}C Dubna (Russia), %	1.1±0.2	0.6±0.2	1.0±0.2	3.2±0.2	5.6±0.2	7.6±0.2	115±2
72 GeV ^{40}Ar Berkeley (USA), %	3.6±0.3	2.2±0.2	3.0±0.9	5.2±0.3	9.0±0.5	13.0±0.6	130±2

Fig. 19. The «2π-Cu target» set-up consisting of two Cu disks ($\varnothing = 8$ cm, $d = 1$ cm) separated by 20 cm together with several in-between Cu rings for the study of wide-angle emission of energetic secondary fragments producing ^{24}Na. The $R_\Theta(^{24}\mathrm{Na})$ values (ratio of ^{24}Na activity in a downstream target and the front disk) for three different irradiations are given in the table below the drawing [4]

The open space between the two disks is filled with several Cu rings serving the study of wide-angle emission of energetic secondary fragments that can produce ^{24}Na in these Cu rings. The target was irradiated with 72 GeV ^{40}Ar in Berkeley (USA), 44 GeV ^{12}C in Dubna (Russia), and 4 GeV ^{4}He at Saclay (France). In Fig. 19 (bottom) the relevant experimental results are shown. The observation of substantial production of ^{24}Na in Cu rings by wide-angle emitted secondary fragments is obvious. The most striking results for the ^{24}Na production by secondary fragments in Cu rings exposed to large angles Θ are as follows.

• There is a definite contribution of yields $R_\Theta^{\mathrm{exp}}(^{24}\mathrm{Na})$ — defined as the ratio of ^{24}Na in a specific Cu ring exposed to idealized lab angles Θ relative

to the ^{24}Na activity in the Cu front plate — in the interval $10 < \Theta < 43^\circ$ for irradiations with 44 GeV ^{12}C and 72 GeV ^{40}Ar. These yields are in the range of a few percent. Only very tiny yields for $R^{\rm exp}_{\Theta}(^{24}{\rm Na})$ are observed in the Cu rings in the interval $43 < \Theta < 90^\circ$. They are due to the beam halo and will not be considered any further.

• Some $R_d(^{24}{\rm Na})$ yields have apparently been «lost» in the two-Cu-disk experiment as described above. In the «2π-Cu target» experiment these «lost» activities have been recovered as $R^{\rm exp}_{\Theta>10}(^{24}{\rm Na})$ in Cu rings exposed to secondary fragments in the angular interval $10 < \Theta < 43^\circ$ for irradiations with 44 GeV ^{12}C and 72 GeV ^{40}Ar. Any true «losses» of ^{24}Na activities would show up as a difference defined as

$$\Delta R^{\rm exp} = R_{d=0}(^{24}{\rm Na}) - \sum_{\Theta=0}^{\Theta=43} R_{\Theta}(^{24}{\rm Na}). \tag{12}$$

Carrying out the proper beam-halo corrections as described in detail [6, 7] one has calculated the following values for $\Delta R^{\rm exp}$:

$$\text{For irradiations with 4 GeV } ^4\text{He [6]: } \Delta R^{\rm exp} = 0.002 \pm 0.014, \tag{13}$$

$$\text{For irradiations with 44 GeV } ^{12}\text{C [6]: } \Delta R^{\rm exp} = 0.01 \pm 0.04, \tag{14}$$

$$\text{For irradiations with 72 GeV } ^{40}\text{Ar [7]: } \Delta R^{\rm exp} = 0.07 \pm 0.03. \tag{15}$$

This quantitative analysis shows that practically no $R_0(^{24}{\rm Na})$ activities are «lost» within the experimental uncertainties in irradiations with 44 GeV ^{12}C and 4 GeV ^{4}He projectiles. Such possibilities of «losses» had been considered in earlier investigations [20, 21] for irradiations of two Cu disks with 72 GeV ^{40}Ar projectiles. This could not be confirmed with certainty in irradiations with 72 GeV ^{40}Ar, as the «loss» amounts only $(7 \pm 3)\%$.

• Theoretical estimates of particle spectra of secondary fragments emitted into large lab angles $\Theta \geqslant 10^\circ$ show that practically only protons, neutrons, and pions are emitted into these large angles. This result has been experimentally confirmed in studies using nuclear emulsions exposed to relativistic heavy ions [21]. Studies using solid-state-nuclear-track detectors (SSNTD) gave additional experimental confirmation of this claim [5]. As the excitation function for the production of ^{24}Na in thin Cu targets is well known [2, 6, 21], it is possible to calculate the $R^{\rm cal}_{(10<\Theta<43)}$ yields for ^{24} Na activities in Cu rings. The calculations are based on the Dubna DCM/CEM code [23] and they yield in comparison with the experimental value $R^{\rm exp}_{(10<\Theta<43)}$ for ^{24} Na activities always statistically significant lower yields:

For irradiations with 44 GeV ^{12}C [5, 6, 8]:

$$R^{\rm cal}_{(10<\Theta<43)} \leqslant 0.02 \longleftrightarrow R^{\rm exp}_{(10<\Theta<43)} = 0.11 \pm 0.02. \tag{16}$$

For irradiations with 72 GeV ^{40}Ar [7]:

$$R^{\mathrm{cal}}_{(10<\Theta<43)} \leqslant 0.02 \longleftrightarrow R^{\mathrm{exp}}_{(10<\Theta<43)} = 0.19 \pm 0.02. \tag{17}$$

Calculations of $R^{\mathrm{cal}}_{(10<\Theta<43)}$ in 72 GeV ^{40}Ar irradiation have also been carried out by Lerman [2] with the same result. One observes a striking and significant difference between the observation and calculations for wide lab angles with $\Theta \geqslant 10^{\circ}$. The calculations give always $\leqslant 2\%$ of the ^{24}Na activity in the Cu rings exposed to these angles, the observations give $(11 \pm 2)\%$, resp. $(19 \pm 2)\%$ of the ^{24}Na activity in the same angular interval. This is another aspect of «unresolved enhancement effects» for short linear ranges of dimensions between about 5 up to 20 cm in Cu targets, as this is the distance between the Cu front plate and the respective Cu rings within the «2π-Cu target».

One further aspect shall be described here. The results from Fig. 19 indicate that the intensity of wide-angle emission of secondary particles scales with the total energy E of the projectile. This shall be demonstrated by looking into the $R_d(^{24}\mathrm{Na})$ results discussed earlier in Sec. 2. These results were obtained with the two Cu disk configuration at $d = 0$ cm (i.e., in contact) registering all secondary fragments emitted forward into the second Cu disk. With the configuration at $d = 20$ cm distance only fragments have been registered in the second Cu disk which are emitted into angles $\Theta < 10^{\circ}$ in the forward direction. One can define for ^{24} Na activities a value $\Delta R_d(E)$ for a specific projectile at a given E and two different distances between two Cu disks with $d = 0$ cm and $d = 20$ cm (or 10 cm in some experiments):

$$\Delta R_{d=20 \text{ or } 10}(E) = \frac{(R_0(^{24}\mathrm{Na}) - R_{d=20 \text{ or } 10}(^{24}\mathrm{Na})}{R_0(^{24}\mathrm{Na})} \tag{18}$$

giving the results for ^{40}Ar irradiations [21]:

$$\Delta R_{d=20}\,(72\ \mathrm{GeV}) = (16.1 \pm 2.2)\%, \tag{19}$$

$$\Delta R_{d=20}\,(36\ \mathrm{GeV}) = (2.2 \pm 2.8)\%, \tag{20}$$

for ^{12}C irradiations [6]:

$$\Delta R_{d=20}\,(44\ \mathrm{GeV}) = (9.3 \pm 3.3)\%, \tag{21}$$

$$\Delta R_{d=10}\,(44\ \mathrm{GeV}) = (5.6 \pm 0.4)\%, \tag{22}$$

$$\Delta R_{d=10}\,(25\ \mathrm{GeV}) = (1.7 \pm 2.1)\%, \tag{23}$$

and for ^{4}He irradiations [6]:

$$\Delta R_{d=20}\,(4\ \mathrm{GeV}) = (1.0 \pm 1.6)\%. \tag{24}$$

The effect defined with $\Delta R_{d=20 \text{ or } 10}(E)$ appears to scale with the total energy, E, of the primary projectile. These results have also been published in [6, 21]. A similar scaling with the total energy, E, of the projectile had already been presented for $R_0^{\exp}(^{24}\text{Na})$ in Fig. 17, *b*.

As mentioned already, only protons, neutrons, or even pions are emitted into large lab angles with $\Theta > 10^\circ$. This implies that these p, n, and π may have — at least partially — an unexpected behaviour. When their kinetic energy is measured experimentally, for example, in bubble chambers (references can be found in [20, 21]), their kinetic energy is rather low and well-understood with model calculations. But one could not match the model calculations with the experimental findings for $R^{\exp}_{(10<\Theta<43)}(^{24}\text{Na})$. Unfortunately, the direct experimental evidence for a change in the angular distribution of energetic secondary fragments at large lab angles with respect to a change in the total energy, E, of the primary projectile was missing. This challenging question has been answered in a quantitative and independent manner by Kulakov et al. [33]. They investigated experimental results observed directly for (quote [33]): «fast secondary particles produced in ^{12}C interactions at relativistic energies». Nuclear interactions induced by 15.1 GeV ^{12}C and 41.5 GeV ^{12}C were studied with a propane bubble chamber. In this case, mostly C + C and C + H interactions were observed and compared with (C + Cu) interactions studied radiochemically. To be precise, one observes secondary fragments and measures their momentum in the magnetic field of the propane chamber via the curvature of their tracks. The experimental results from the propane chamber were kindly presented by the staff of the Chamber Division at the Laboratory of High Energies of the Joint Institute for Nuclear Research in Dubna. The results of their data analysis lead to the following conclusion:

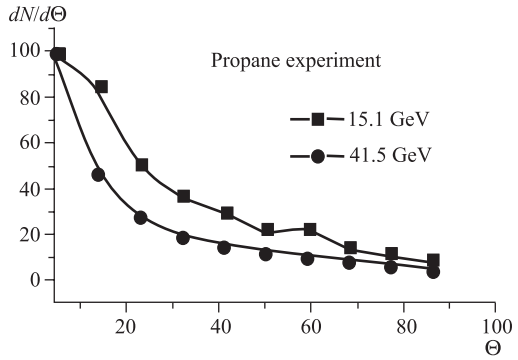

Fig. 20. The angular distribution of fast ($E > 1$ GeV) secondary protons produced by 15.1 and 41.5 GeV ^{12}C, respectively. One observes $\approx 40\%$ of all fast secondary protons outside the angle $\Theta > 19^\circ$ for 15.1 GeV ^{12}C, however, only $\approx 22\%$ of all fast secondary protons outside the angle $\Theta > 19^\circ$ for 41.5 GeV ^{12}C. The radiochemical evidence for the production of ^{24}Na shows just the opposite trend [33]

• No large difference in the angular distribution for fast secondary fragments is observed experimentally when nuclear interactions of 15.1 and 41.5 GeV ^{12}C ions in a propane bubble chamber are compared. If there is any difference at all, we may observe a few more fast secondaries at 15.1 GeV emitted into large lab angles as compared to 41.5 GeV ^{12}C ions, as shown in Fig. 20. Rather similar results have been observed when comparing nuclear interactions of 36 and 72 GeV ^{40}Ar in nuclear emulsion [21].

Experimental findings about product yields in experiments with thick Cu targets are in contrast to the bubble chamber results:

• A difference of the ^{24}Na yield produced by secondary fragments in copper at large angles ($\Theta > 19°$) has been observed, where less ^{24}Na is produced by 25 GeV ^{12}C than by 44 GeV ^{12}C (see Eqs. (22), (23)). The effect has a statistical significance by nearly two standard deviations. A similar enhancement has been observed in nuclear interactions of 36 and 72 GeV ^{40}Ar in copper. In this latter case the statistical evidence was much more significant (see Eqs. (19), (20)).

The difference of the two above experimental observations is again another aspect of unresolved problems, as already discussed [6, 21].

Finally, it should be mentioned, that this paper is not a complete list of all the experiments carried out in these studies between 1980 up to about the year 2000. The interested reader can find further experiments with various Cu-target configurations in the PhD thesis of Heck [7], published in [6].

5.2. The Production of Several Isotopes in Cu Rings of the Diluted «2π-Cu Target». An observation at large lab angles $\Theta \geqslant 10°$ shall be discussed for the first time in a publication, which has been reported so far only in the PhD thesis of F. Pille at the former Technische Hochschule Leipzig, Germany [8]. Due to the well-focussed beams of the Saturne and Synchrophasotron accelerators one did observe practically no yields of ^{24}Na ($R_\Theta(^{24}\text{Na}) \leqslant 1\%$) in copper rings in the angular range $52 < \Theta < 90°$ in irradiations with 4 GeV ^{4}He and 44 GeV ^{12}C as shown in Fig. 19. The Cu rings for the angles $52 < \Theta < 90°$ are rather free of activation products besides ^{58}Co. The Cu rings in the range $10 < \Theta < 52°$ do register nuclear reaction products that are produced by secondary fragments emitted into these angular intervals from the front Cu disk. The resulting yields for product nuclides, such as ^{58}Co, ^{44}Sc, and ^{24}Na in Cu rings at large angles have been recorded in this study. This yields, for example, the limited «three-point mass yield curves» in specific angles (i.e., Cu rings) are shown in Fig. 21 for the irradiation with 4 GeV He^4 ions.

Within the angular interval $43 < \Theta < 52°$ the observed mass yield curve has just the shape as expected for an irradiation of copper by low-energy hadrons with energy close to 100 MeV. One observes predominantly the close by-product ^{58}Co and hardly any other induced activities. This finding agrees qualitatively with theoretical expectations.

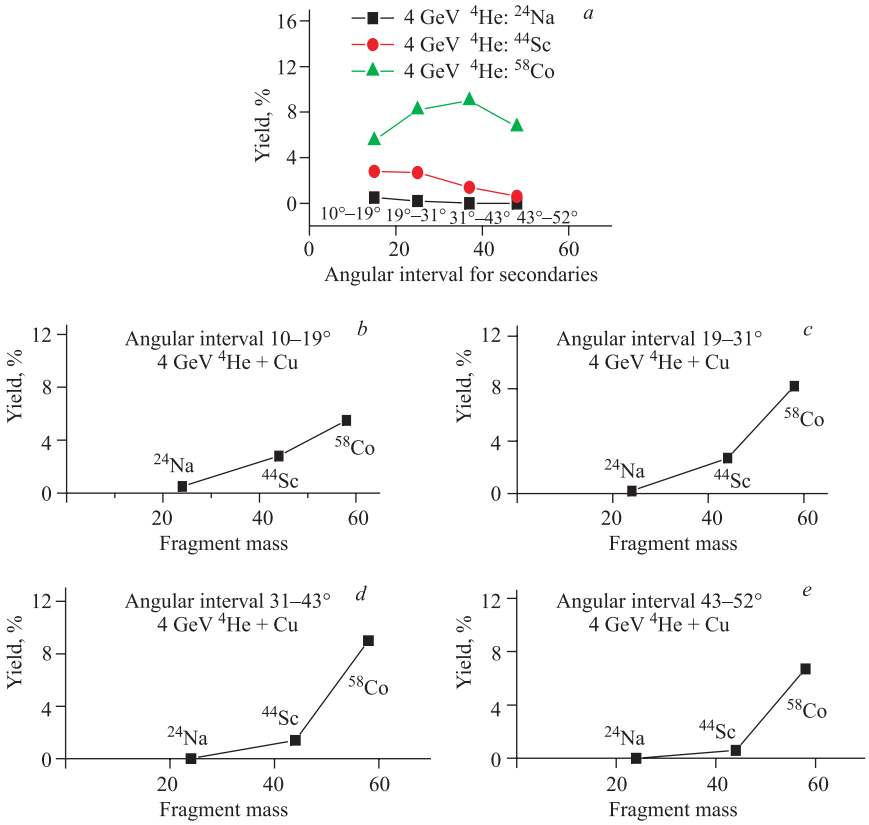

Fig. 21. «Three-point mass yield curves» in specific Cu rings induced by secondary fragments produced by 4 GeV ^{4}He in copper. Secondary fragments are emitted into large lab angles, where they interact with Cu rings of the diluted «2π-Cu target» [8]. The yield for a specific isotope in a given Cu ring is the ratio of its activity in the ring compared to the front disk in %. The experimental uncertainty is about 20%. Details are given in the text

In the angular interval $10 < \Theta < 19^{\circ}$ the observed mass yield curve has the shape as expected for an irradiation in thin copper by low-energy hadrons with energy of several 100 MeV. One observes the close by-product ^{58}Co, but in addition some smaller amount of ^{44}Sc activity and very little other products with a smaller mass, including ^{24}Na. This finding agrees well with theoretical expectations. The two other mass yield curves in-between $19 < \Theta < 43^{\circ}$ are just «in-between».

The mass yield curve in specific copper rings produced by secondary fragments which are produced in nuclear reactions of 44 GeV ^{12}C in copper is shown

in Fig. 22. There are some significant differences in comparison with Fig. 21. The observed mass yield curve in the angular interval $43 < \Theta < 52°$ has again the shape as expected for an irradiation of copper with hadrons with energy of a few 100 MeV. One observes predominantly the close by-product ^{58}Co, the activity of ^{44}Sc is reduced, and ^{24}Na is barely observed at all. This again agrees well with expectations.

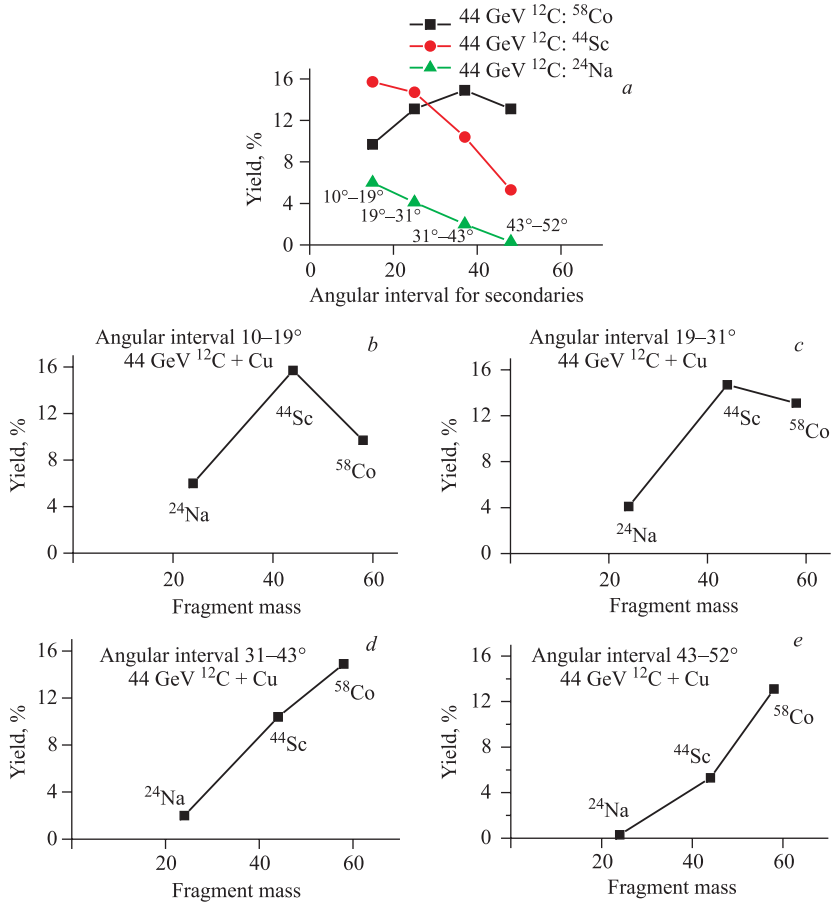

Fig. 22. «Three-point mass yield curves» in specific Cu rings induced by secondary fragments produced by 44 GeV ^{12}C in copper. The secondary fragments are emitted into large lab angles, where they interact with specific Cu rings of the diluted «2π-Cu target» [8]. The yield for a specific isotope in a given Cu ring is the ratio of its activity in the ring as compared to the front disk in %. The experimental uncertainty is about 20%. Details are given in the text

However, the observed mass yield curve in the angular interval $10 < \Theta < 19°$ has the same unexpected shape as observed in the irradiation of the massive 20 cm thick copper block with 44 GeV ^{12}C shown in Fig. 3. ^{44}Sc is produced with a larger relative abundance than ^{58}Co, and the isotope ^{24}Na is produced in substantial yield. More precise: The activity of the isotope ^{A}Z in the ring is given in % of the activity in the Cu front plate for the same isotope ^{A}Z. This finding disagrees with theoretical expectations — however, this time it is also observed for secondary fragments emitted as projectiles into large lab angles. According to our knowledge, such secondary particles must be either protons, neutrons, or pions. As the observed cross sections are quite dominant, it is very unlikely that they are induced by small contribution of deuterons or tritons in the flux of secondary fragments at large angles.

It has been shown that alphas or larger particles can be excluded from inducing the observed effect [5, 21, 32]. This phenomenon of excessive production of products with large ΔA constitutes another and rather severe aspects of unresolved problem as this effect is most likely due to elementary particles like protons, neutrons, or even pions. The two angular intervals in-between $19 < \Theta < 43°$ show an intermediate behaviour.

Theoretical model calculations have been carried out for the 4 GeV ^{4}He irradiation of the «2π-Cu target» according to [19]. The set-up exactly as described in Fig. 19 is built into the code (MCNPX) and the irradiation with 4 GeV ^{4}He ions is simulated. The resulting fluences for neutrons, protons, pions, deuterons, tritons, and alphas in different Cu rings of the set-up corresponding to different angles have been calculated. Typical results for the most abundant secondary particle, i.e., neutrons, in different angular rings are shown in Fig. 23. The total neutron fluence is separated into two energy intervals. The fluence for «low»

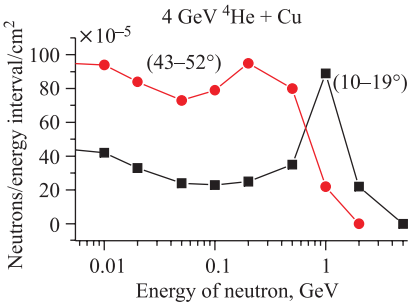

Fig. 23. The calculated neutron energy spectra entering two different Cu rings. Further details are given in the text

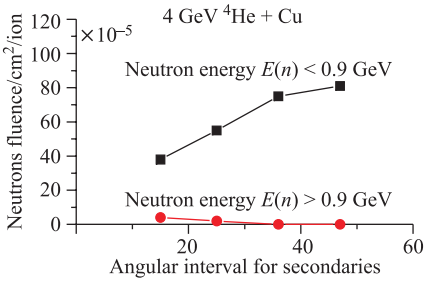

Fig. 24. The calculated «low» and «high» energy neutron fluence in different angular intervals shown in Fig. 19. Details are given in the text

energy neutrons with $E(n) < 0.9$ GeV is responsible for the dominant production of the «close-by» spallation product ^{58}Co from ^{63,65}Cu. This calculated fluence is only slightly angular-dependent, just as the experimental distribution of ^{58}Co shown in Fig. 21, *a*. In contrast to this, the fluence for «high» energy neutrons with $E(n) > 0.9$ GeV is predominantly responsible for the production of the fragmentation product ^{24}Na from Cu, which is produced with a threshold around 0.9 GeV. The theoretical fluence is much smaller, just as the corresponding experimental production of ^{24}Na shown in Fig. 21, *a*. Obviously, the tiny yields ($\approx 0.1\%$) for ^{24}Na at very large angles $\Theta > 52^\circ$ cannot be explained by this calculation; they are due to the experimental beam halo.

The calculated secondary neutron energy spectra entering the Cu rings at angular ranges ($10 < \Theta < 19^\circ$) and ($43 < \Theta < 52^\circ$) are shown in Fig. 24. The energy distribution at the smaller angles is centered around 1 GeV and these neutrons have considerably higher energy than neutrons emitted at larger angles. This calculation supports, in particular for energies ($E > 0.9$ GeV), the earlier qualitative statements explaining the «three point mass yield curves» produced by 4 GeV ^{4}He ions.

Similar calculations are available for the reaction of 44 GeV ^{12}C on the diluted «2π-Cu target» [6, 8]. The mean kinetic energies and the respective fluences for p, n, and π are calculated with the Dubna Cascade Model, including coalescence and precompound model components. The mean energy for p and n is around 1 GeV in the interval $10 < \Theta < 19^\circ$ — quite similar to the 4 GeV ^{4}He case. The effects shown in Fig. 22, however, remain unexplained.

Finally, it should be mentioned that rather similar effects have been observed in the first «two-Cu-disks» experiments irradiated with 72 GeV ^{40}Ar at the Bevalac, described by Aleklett et al. [21] and reviewed in Sec. 2 and Fig. 6. The downstream Cu disk is surrounded by a Cu ring, both at the $d = 0$ cm and $d = 20$ cm distances (Fig. 6, *a*). This ring in the $d = 0$ cm configuration is sensitive to the beam halo and at $d = 20$ cm distance additionally to ($Z \leqslant 1$) secondaries from the front plate emitted into lab angles Θ with $10 < \Theta < 20^\circ$. These configurations are not as clear-cut geometrically as the diluted «2π-Cu target» (Fig. 19), as the back-end Cu disk is farther away from the ring in the later configuration. Nevertheless, both arrangements are rather similar. The results are shown in Table 4.

The yields for $d = 0$ cm are due to interactions of the primary beam halo in a thin target and show the classical behavior of a yield distribution according to the concept of «limiting fragmentation», i.e., low yields for $A < 30$, and a steady increase of the yields from ^{46}Sc up to ^{58}Co by a factor of 4. The yield distribution for $d = 20$ cm shows a rather similar behavior as observed earlier in Fig. 22 in the same angular interval with $10 < \Theta < 20^\circ$ for irradiations with 44 GeV ^{12}C, i.e., relatively high yields for $A < 30$, and rather constant yields from ^{46}Sc up to ^{58}Co. Obviously, the energy spectrum of the calculated

Table 4. **Relative yields R^* of different nuclides in downstream Cu rings (Fig. 6, a) after the irradiation with 72 GeV ^{40}Ar [21]**

Isotope	R (ring at $d = 0$ cm)	R (ring at $d = 20$ cm)
^{7}Be	< 0.02	0.072±0.013
^{24}Na	< 0.01	0.071±0.005
^{28}Mg	< 0.01	0.060±0.010
^{46}Sc	0.015±0.003	0.159±0.007
^{54}Mn	0.041±0.002	0.174±0.007
^{56}Co	0.054±0.003	0.169±0.007
^{58}Co	0.065±0.003	0.168±0.006

Note. The Cu ring at $d = 20$ cm is also sensitive to ($Z \leqslant 1$) secondaries emitted with $10 < \Theta \leqslant 19^\circ$ from the front Cu plate. Details are given in the text.

* R is the ratio of the activity in the ring as compared to the front plate.

fluence of ($Z \leqslant 1$) secondaries produced by 72 GeV ^{40}Ar (Fig. 8) with its strong component of low-energy ($Z \leqslant 1$) secondaries should have given a very strong increase in the production of spallation products close to the Cu target. One would have expected a large yield for the production of ^{58}Co. But this has not been observed experimentally. This is again another aspect of unresolved problems for interactions of 72 GeV ^{40}Ar in thick targets at the Bevalac.

But the open question mentioned at the end of the preceding Sec. 4 can be answered in the following way: «Minimum ionizing particles» produced among secondary ($Z \leqslant 1$) fragments in nuclear interactions of ions with a total energy $E > 30$ GeV have also an «enhanced nuclear destruction ability», at least, when they are emitted into wide agles with $10 < \Theta < 19^\circ$.

6. COMPARISON OF «WIDE-ANGLE EFFECTS» IN NUCLEAR EMULSIONS WITH RADIOCHEMICAL STUDIES OF ^{24}Na IN Cu

A Response to a Critical Paper by Tolstov [34]. The evidence for another aspect of an unresolved problem is presented in Fig. 25. The angular distribution of «minimum ionizing particles» $dN^{\exp}/d(\Theta)$ is shown in Fig. 25, c, d observed for secondaries in nuclear emulsions irradiated with 72 GeV ^{40}Ar and 44 GeV ^{12}C. $dN^{\exp}/d(\Theta)$ is defined as the number of relativistic secondary protons with energy $E_P > 375$ MeV or pions with energy $E_\pi > 56$ MeV emitted into the lab angle θ. In addition, the experimentally observed angular distribution of $R_\Theta^{\exp}(^{24}\text{Na})$ in rings of the diluted «2π-Cu target» is shown in Fig. 25, a, b.

One observes a similar decrease for the $dN^{\rm exp}/d(\Theta)$ distribution of «minimum ionizing particles» as well as for the $R_\Theta^{\rm exp}(^{24}{\rm Na})$ yields in copper rings in these two heavy-ion irradiations.

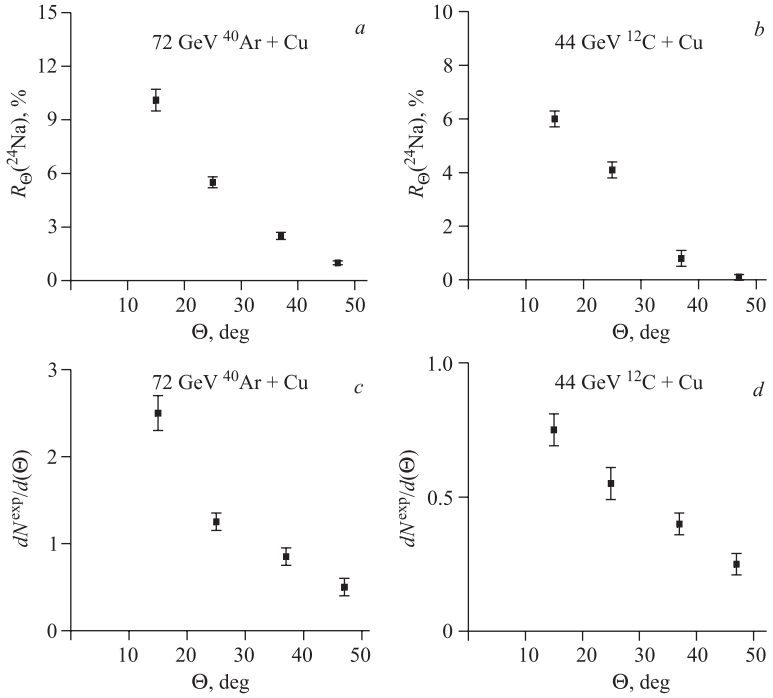

Fig. 25. The angular distribution of secondary «minimum ionizing particles», $dN^{\rm exp}/d(\Theta)$, in nuclear emulsions irradiated with 72 GeV ^{40}Ar (a, c) and 44 GeV ^{12}C (b, d) is shown together with the angular distribution of $R_\Theta^{\rm exp}(^{24}{\rm Na})$ yields in rings of the diluted «2π-Cu target» as shown in Fig. 19 [34, 35]. a, b) The angular distribution of $R_\Theta^{\rm exp}(^{24}{\rm Na})$ yields in rings of the «2π-Cu target». c, d) The angular distribution of secondary «minimum ionizing particles», $dN^{\rm exp}\ /d(\Theta)$

This similarity in the decrease with the angle Θ for both distributions is an experimental fact. Tolstov [34] noted this similarity and concluded that exactly this similarity in the decrease with the angle Θ explains in a simple manner the experimental facts shown in Fig. 25, as shown below in Table 5 for irradiations with 72 GeV ^{40}Ar:

$$\frac{R_\Theta^{\rm exp}(^{24}{\rm Na})}{dN^{\rm exp}/d(\Theta)} = (3.9 \pm 0.2)\% \quad \text{for} \quad 11 < \Theta < 19^\circ, \tag{25}$$

$$\frac{R_\Theta^{\rm exp}(^{24}{\rm Na})}{dN^{\rm exp}/d(\Theta)} = (4.4 \pm 0.5)\% \quad \text{for} \quad 19 < \Theta < 31^\circ. \tag{26}$$

Table 5. **Experimental $R_{\Theta}^{\exp}(^{24}\mathrm{Na})$ and calculated $R_{\Theta}^{\mathrm{cal}}(^{24}\mathrm{Na})$ yields observed in Cu rings and the angular distribution $dN^{\exp}/d(\Theta)$ for «minimum ionizing particles» observed in nuclear emulsions during irradiations with 72 GeV ^{40}Ar [7]**

Parameters	$11 < \Theta < 19^{\circ}$	$19 < \Theta < 31^{\circ}$	$31 < \Theta < 43^{\circ}$
$R_{\Theta}^{\exp}(^{24}\mathrm{Na})$, %	5.5 ± 1.0	3.7 ± 0.8	1.4 ± 0.5
$R_{\Theta}^{\mathrm{cal}}(^{24}\mathrm{Na})$, %	0.94 ± 0.15	0.43 ± 0.07	0.15 ± 0.02
$dN^{\exp}/d\ (\Theta)$	0.75	0.57	0.39
$\frac{R_{\Theta}^{\exp}(^{24}\mathrm{Na})}{dN^{\exp}/d(\Theta)}$, %	7.3 ± 1.2	6.4 ± 1.2	3.6 ± 1.2
$\frac{R_{\Theta}^{\mathrm{cal}}(^{24}\mathrm{Na})}{dN^{\exp}/d(\Theta)}$, %	1.2 ± 0.2	0.75 ± 0.15	0.38 ± 0.08
$\frac{R_{\Theta}^{\exp}(^{24}\mathrm{Na})}{R_{\Theta}^{\mathrm{cal}}(^{24}\mathrm{Na})}$	5.8 ± 1.5	8.6 ± 2.6	9 ± 3

But this interpretation of Tolstov implied that the *energy spectra for «minimum ionizing particles» are being invariant with respect to the angle* θ for secondary fragments in the angular interval $11 < \Theta < 31^{\circ}$. With this assumption he could explain the *constant ratios* in Eqs. (25) and (26).

However, this disagrees with the well-known and fundamental results from all studies of the energies of secondary particles emitted into various lab angles. As the transverse momentum of these particles is angle-independent, their lab energy must increase with decreasing lab angle. More quantitative calculations have been given elsewhere [6–8, 20]. A detailed look into Table 5 shows that the model calculated values of $R_{\Theta}^{\mathrm{cal}}(^{24}\mathrm{Na})$ are definitely angular-dependent:

$$\frac{R_{\Theta}^{\mathrm{cal}}(^{24}\mathrm{Na})}{dN^{\exp}/d(\Theta)} = (0.64 \pm 0.07)\% \quad \text{for} \quad 11 < \Theta < 19^{\circ}, \tag{27}$$

$$\frac{R_{\Theta}^{\mathrm{cal}}(^{24}\mathrm{Na})}{dN^{\exp}/d(\Theta)} = (0.43 \pm 0.05)\% \quad \text{for} \quad 19 < \Theta < 31^{\circ}. \tag{28}$$

This contradicts the simplified description of Tolstov, as the calculated difference in the two angular intervals is about two standard deviations. This forced some authors [35] (including Tolstov himself) to reject this simple interpretation of Tolstov [34]. The energies for «minimum ionizing particles» decrease when going from the interval $10 < \Theta < 20^{\circ}$ to the larger angular interval $20 < \Theta < 30^{\circ}$ with the consequence of a drastically reduced production cross section of ^{24}Na in Cu by «minimum ionizing particles» [6, 21].

Table 6. **Experimental $R_{\Theta}^{\exp}(^{24}\mathrm{Na})$ and calculated $R_{\Theta}^{\mathrm{cal}}(^{24}\mathrm{Na})$ yields observed in Cu rings and the angular distribution $dN^{\exp}/d(\Theta)$ for «minimum ionizing particles» observed in nuclear emulsions during irradiations with 44 GeV ^{12}C [6]**

Parameters	$11 < \Theta < 19^{\circ}$	$19 < \Theta < 31^{\circ}$	$31 < \Theta < 43^{\circ}$
$R_{\Theta}^{\exp}(^{24}\mathrm{Na})$, %	10.1 ± 0.6	5.5 ± 0.3	2.5 ± 0.2
$R_{\Theta}^{\mathrm{cal}}(^{24}\mathrm{Na})$, %	1.68 ± 0.11	0.54 ± 0.10	0.08 ± 0.02
$dN^{\exp}/d\ (\Theta)$	2.6 ± 0.2	1.25 ± 0.12	0.86 ±0.10
$\frac{R_{\Theta}^{\exp}(^{24}\mathrm{Na})}{dN^{\exp}/d(\Theta)}$, %	3.9 ±0.2	4.4 ±0.5	2.9 ± 0.4
$\frac{R_{\Theta}^{\mathrm{cal}}(^{24}\mathrm{Na})}{dN^{\exp}/d(\Theta)}$, %	0.64 ±0.07	0.43 ± 0.05	0.09 ± 0.02
$\frac{R_{\Theta}^{\exp}(^{24}\mathrm{Na})}{R_{\Theta}^{\mathrm{cal}}(^{24}\mathrm{Na})}$	6.0 ±0.9	10 ±1	30 ± 6

Similar effects observed in the study of nuclear reactions induced by 44 GeV ^{12}C ions are presented in Table 6.

The difference between large experimental yields $R_{\Theta}^{\exp}(^{24}\mathrm{Na})$ and considerably smaller theoretical yields $R_{\Theta}^{\mathrm{cal}}(^{24}\mathrm{Na})$ has already been noted for the entire angular interval $10 < \Theta < 43^{\circ}$ in Eqs. (16), (17). This forces us to conclude, that constant ratios $[R_{\Theta}^{\exp}(^{24}\mathrm{Na})]/[dN^{\exp}/d(\Theta)]$ in the angular interval of $11 < \Theta < 31^{\circ}$ constitute another aspect of unresolved problems in this article.

CONCLUSIONS

Several unresolved problems have been identified in the experimental study of interactions induced by high-energy heavy ions with a total energy above 30 GeV in thick Cu and Pb targets and in nuclear emulsions. All these problems are connected with a stronger energy deposition (*albeit*: destruction ability) of secondary fragments as compared to their primary projectiles. The main experiments have been carried out with 44 GeV ^{12}C at the Synchrophasotron (JINR, Dubna) and with 72 GeV ^{40}Ar at the Bevalac (LBL, Berkeley). The results shall be enumerated in a short form:

1. The radiochemical analysis of interactions of secondary fragments produced in thick targets shows that these secondary fragments excite target nuclei stronger than primary ions. This effect is statistically significant and it has been shown in detail.

In the irradiation of two Cu disks ($\varnothing = 8.0$ cm, $d = 1.0$ cm) in contact with 72 GeV ^{40}Ar one observes in the second Cu disk $(50 \pm 2)\%$ more ^{24}Na than in the first disk. Most advanced model calculations predict no increase exceeding $(0 \pm 2)\%$ for the yield of ^{24}Na in the second Cu disk [1, 2].

The mass yield curve in the second Cu disk compared with that in the first Cu disk obtained in the irradiation with 72 GeV ^{40}Ar does not show any strong increase in the production of spallation fragments with masses above about 55 in the second Cu disk. This finding is inconsistent with model calculations that predict a very abundant production of 100–200 MeV secondary hadrons which should abundantly produce spallation products in the mass range above 55 and close to ^{63,65}Cu target. The same phenomena are observed in experiments with 44 GeV ^{12}C.

Comparing yields of all product masses A of the second Cu disk with the first disk in the irradiations with 36 GeV ^{40}Ar and 72 GeV ^{40}Ar, one observes a strong yield increase in the second disk in the mass interval $7 \leqslant A \leqslant 50$ only for the 72 GeV ^{40}Ar irradiation. Such an increase is not observed for larger product masses above $A > 50$, i.e., close to the target mass.

2. The observation of «more-than-linear» enhancement of neutron production with rising bombarding energy in the irradiation of thick Pb targets with 12 GeV ^{12}C beams and 44 GeV ^{12}C beams was shown first by Vassilkov and his co-workers [10]. This effect was confirmed later by Tolstov [27], and further this effect was confirmed for thick Cu and Pb targets, as reported in this paper. However, the original work of Vassilkov has priority, especially because he presented additionally the most significant results.

3. In the irradiation of the diluted «2π-Cu target» with 44 GeV ^{12}C and 72 GeV ^{40}Ar one observes the emission of secondary particles that produce substantial yields of ^{24}Na in Cu at large lab angles $10 < \Theta < 43^\circ$. The enhancement of these experimental yields as compared to model calculations amounts to nearly one order of magnitude. Some further details appear to be remarkable.

The «three-point mass yield curve» in a Cu ring placed at lab angles $10 < \Theta < 19^\circ$ in the irradiation with 44 GeV ^{12}C of a Cu target has a completely unexpected shape: only a little ^{58}Co is produced, however, much more ^{44}Sc and surprisingly more ^{24}Na. The same effect has been observed in irradiations with 72 GeV ^{40}Ar. Such an effect has not been observed in 4 GeV ^{4}He irradiations.

The ratio of the angular distribution for «minimum ionizing particles», $\dfrac{dN^{\exp}}{d(\Theta)}$, divided by the yields for wide-angle emitted ^{24}Na, $R_{\Theta}^{\exp}(^{24}\mathrm{Na})$, is constant within two angular intervals $11 < \Theta < 19^\circ$ and $19 < \Theta < 31^\circ$ for irradiations with 44 GeV ^{12}C and 72 GeV ^{40}Ar. This is in contrast to theoretical model calculations showing a significant decrease in the calculated yields for $R_{\Theta}^{\mathrm{cal}}(^{24}\mathrm{Na})$ with increasing lab angle.

4. The average number, $\langle N_b \rangle$, of «black prongs» per event (i.e., protons with $E < 30$ MeV) along sequences of nuclear interactions from 72 GeV ^{22}Ne ions in nuclear emulsion was studied. Selected first interactions with at least one ($Z \geqslant 2$) projectile fragments gave $\langle {}^1N_b \rangle_{\rm sel} = 4.56 \pm 0.27$. On the average all interaction of ($Z \geqslant 2$) projectile fragments gave a significantly larger number, $\langle {}^2N_b \rangle = 7.42 \pm 0.60$. This ratio $\langle {}^2N_b \rangle / \langle {}^1N_b \rangle_{\rm sel} = 1.63 \pm 0.16$ is significantly larger than unity. First nuclear interactions without the production of any ($Z \geqslant 2$) projectile fragment must be studied further in detail by several independent methods. This holds, in particular, in view of point 3 (above). The developed nuclear emulsion method of N_b measurements is a perspective instrument additional to the radiochemical method to study thick targets and further experiments should be requested.

It has not been the intention of this paper to suggest a solution for the understanding of these unresolved problems. One possible (or unlikely?) way to understand the experimental phenomena can be found elsewhere [26]. However, it is of interest to speculate about several practical and socio-economical applications [12]:

• Enhanced transmutation capacity for the destruction of plutonium (Pu $\rightarrow$ fission fragments) with high-energy relativistic ions.

• Enhanced breeding capacity for the production of plutonium (U $\rightarrow$ Pu) using high-energy relativistic ions.

• The observation of excess neutron production in 44 GeV ^{12}C irradiations may give access to hitherto unknown energy reservoirs.

• The activation in the Cu ring at angles $10 < \Theta < 19^\circ$ and exposed to ≈ 1 GeV ($Z \leqslant 1$) secondaries yields in the irradiation of the «2π-Cu target» with 44 GeV ^{12}C more ^{44}Sc than ^{58}Co (Fig. 22). Such an effect is not known from any relativistic primary hadron irradiating thin Cu targets with energies up to 300 GeV. This may indicate an «information transfer» within hitherto unknown media. Protons, neutrons (or pions) emitted into large lab angles have a relatively *low measured momentum,* however, they can transfer *enhanced nuclear «destruction ability»* over distances of at least 20 cm.

Acknowledgements. This work has been carried out within a broad international cooperation of many scientists and their home institutions over nearly 25 years. It is impossible to mention all of them, but it is important to remember that the late Professor E. M. Friedlander (LBL, Berkeley, USA) initiated this research. Decades of support through the Laboratory of High Energies (JINR, Dubna, Russia) by the late Academician A. M. Baldin is deeply acknowledged, as well as the strong and continued help of Director Professor A. I. Malakhov and Professor A. D. Kovalenko and their staff.

REFERENCES

1. *Brandt R.* Do We Really Understand Nuclear Reactions within Thick Targets Using GeV-Hadrons? // Radiat. Meas. 2003. V. 36. P. 249–259.
2. *Lerman L.* On the Symmetry of Nuclear Identity between Relativistic Primary and Secondary Nuclei. Diss. Marburg: Philipps-Univ., 2002 (Universitäts-Bibliothek. Digital dissertation: Sign. 4^0Z 2002/0105).
3. *Ochs M.* Experimente zur Neutronenfreisetzung durch Spallationsreaktionen in massiven Kupfer- und Blei-Targets. Diss. Marburg: Philipps-Univ., 1997.
4. *Brandt R. et al.* Search for New Phenomena in High-Energy Heavy Ion Interactions // Nucl. Tracks Radiat. Meas. 1988. V. 15. P. 383–392.
5. *Brandt R. et al.* Wide Angle Emission of Heavy Fragments in Relativistic Heavy Ion Collisions and Some Open Problems // Nucl. Track Radiat. Meas. 1993. V. 22. P. 537–546.
6. *Brandt R. et al.* Enhanced Production of ^{24}Na by Wide-Angle Secondaries Produced in the Interaction of Relativistic Carbon Ions with Copper // Phys. Rev. C. 1992. V. 45. P. 1194–1208.
7. *Heck M.* Weitwinkelemission energiereicher Sekundärteilchen bei der Wechselwirkung relativistischer Schwerionen mit Kupfertargets. Diss. Marburg: Philipps-Univ., 1992.
8. *Pille F.* Untersuchungen zum Verhalten leichter relativistischer Projektilfragmente. Diss. Leipzig: Techn. Hochschule, 1989.
9. *Brandt R. et al.* Further Evidences for Enhanced Nuclear Cross-Sections Observed in 44 GeV Carbon Ion Interactions with Copper. JINR Preprint E1-95-502. Dubna, 1995.
10. *Vassilkov R. G. et al.* Neutron Yields from Bulky Lead Targets under Action of Relativistic Ions // At. Energy. 1995. V. 79. P. 257–264;
Vassilkov R. G. et al. On Electronuclear Breading // Usp. Fiz. Nauk. 1983. V. 139. P. 435.
11. *Brandt R.* Some Contributions from SSNTD towards Nuclear Science; from Multifragmentation towards Accelerator Driven Systems (ADS) // Radiat. Meas. 2001. V. 34. P. 211–219.
12. *Brandt R. et al.* Accelerator Driven Systems (ADS) for Transmutation and Energy Production: Their Challenges and Dangers // Kerntechnik. 2004. Bd. 69. S. 37–50.
13. *Ditlov V. A. et al.* Study of Number of Black Prongs for Two Generations after Nuclear–Nuclear Interactions of 72 GeV ^{22}Ne in Nuclear Emulsion // Proc. of the 22nd Intern. Conf. on Nuclear Tracks in Solids, Barcelona, Spain, Aug. 23–27, 2004.
14. *Cumming J. B. et al.* Spallation of Copper by 80 GeV ^{40}Ar Ions // Phys. Rev. C. 1978. V. 17. P. 1632–1641.
15. *Friedlander E. M., Friedman A.* Frequency Distribution of Heavy Prongs from High-Energy Stars in Nuclear Emulsions // Nuovo Cim. A. 1967. V. 52. P. 912–917.

16. *Friedlander E. M. et al.* Anomalous Reaction Mean Free Path of Projectile Fragments from Heavy Ion Collisions at 2*A* GeV // Phys. Rev. C. 1983. V. 27. P. 1489.

17. *Ganssauge E.* The Experimental Status of the Anomalon Research // Nucl. Tracks Radiat. Meas. 1988. V. 15. P. 371; Ann. Physik. 1987. Bd. 44. S. 202–246.

18. *Dutta A. et al.* Charge Fragmentation in Cosmic Radiation and the Question of Physical Anomalons // Kerntechnik. 2003. Bd. 68. S. 219–222.

19. *Hendricks J. S. et al.* MCNPX Version 2.5.e. LA-UR-04-0569. Los Alamos Nat. Lab., 2004.

20. *Dersch G. et al.* Unusual Behavior of Projectile Fragments from the Interaction of Copper with Relativistic Ar Ions // Phys. Rev. Lett. 1985. V. 55. P. 1176–1179.

21. *Aleklett K. et al.* Unusual Interaction of Projectile Fragments Produced by Relativistic Ar Ions in Copper. Preprint LBL-22422, 1987; Phys. Rev. C. 1988. V. 38. P. 1658–1673; Erratum: Phys. Rev. C. 1991. V. 44. P. 566.

22. *Lund T. et al.* Charge and Mass Distribution of Products from the Nuclear Interaction Between Copper and 1 GeV ^{12}C // Phys. Lett. B. 1981. V. 102. P. 239–241.

23. *Polanski A., Sosnin A. N., Toneev V. D.* JINR Preprint E2-91-562. Dubna, 1991.

24. *Haase G.* Kernchemische Studien zum ungewöhnlichen Weitwinkelverhalten von Sekundärteilchen in relativistischen Schwerionenreaktionen. Ph. D. Thesis. Marburg: Philipps-Univ., 1990.

25. *Wang Y.-L.* Study of Neutron Emission from Massive Targets at Irradiation with Relativistic Heavy Ions by Nuclear Emulsions and Nuclear Track Detectors. Ph. D. Thesis. Adv. Res. Inst. for Sci. Tokyo: Waseda Univ., 1998.

26. *Brandt R.* Das Konzept der Information nach Szilard und Unger und die beiden Hauptsätze der Thermodynamik in der Elementarteilchenforschung // Math. Phys. Korresp. 2005. Nr. 220. Z. 3–17.

27. *Brandt R.* Measurements of Neutron Yields and Radioactive Isotope Transmutation in Collisions of Relativistic Ions with Heavy Nuclei. JINR Preprint E1-99-251. Dubna, 1999.

28. *Ochs M. et al.* SSNTD and Radiochemical Studies on the Transmutation of Nuclei Using Relativistic Ions // Radiat. Meas. 1997. V. 28. P. 255–268.

29. *Friedlander E. M., Heckmann H. H.* Relativistic Heavy Ion Collisions: Experiment. Preprint LBL-13864; 1982. Heavy Ion Sci. Plenum Press, 1983.

30. *Tolstov K. D.* Complete Destruction of Heavy Nuclei by Hadrons and Nuclei // Z. Phys. A: Atoms and Nuclei. 1981. Bd. 301. S. 339–342.

31. *Khan H. A. et al.* Exceptionally High Multiplicity Events Observed in the Interaction of Relativistic Uranium Ions with Light Target Atoms // Nucl. Instr. Meth. B. 1991. V. 61. P. 497–501.

32. *Arbuzov B. A. et al.* On the SSNTD in Relativistic Heavy Ion Physics and the Study of Open Questions // Nucl. Tracks Radiat. Meas. 1991. V. 19. P. 557–567.

33. *Kulakov B. A. et al.* On the Different Experimental Behavior of Fast Particles Produced in ^{12}C Interactions at Relativistic Energies. JINR Preprint E1-98-51. Dubna, 1998; Kerntechnik. 1998. Bd. 63. S. 249–254.

34. *Tolstov K. D.* On the Anomalon Interpretation of $^{40}Ar + Cu$ Collisions at 0.9 and 1.8A GeV // JINR Rapid Commun. 1987. No. [21]. P. 27; Z. Phys. A. 1989. Bd. 333. S. 79.

35. *Dersch G. et al.* On the Anomalon Interpretation of $^{40}Ar + Cu$ Collisions at 0.9 and 1.8 GeV // Isotopenpraxis. 1989. V. 27. P. 303–304.